Morphological Systems for Multidimensional Signal Processing

PETROS MARAGOS, MEMBER, IEEE, AND RONALD W. SCHAFER, FELLOW, IEEE

This paper reviews the basic theory and applications of a set theoretic approach to image analysis called mathematical morphology. *The goals of the paper are: (1) to show how the concepts of mathematical morphology can quantify geometrical structure in signals and (2) to illuminate the ways that morphological systems can enrich the theory and applications of multidimensional signal processing. The topics covered include: applications to* non-linear filtering *(morphological and rank-order filters, multiscale smoothing, morphological sampling, morphological correlation); applications to* image analysis *(feature extraction, shape representation and description, size distributions, and fractals); and* representation theorems, *which show how a large class of nonlinear and linear signal operators can be realized as a combination of simple morphological operations.*

I. Introduction

Multidimensional signal processing has been based traditionally on the concepts and theory of linear systems and Fourier analysis (or other related transforms) [10], [11], [27], [136]. Although these classical approaches have been very fruitful in many applications, they are often of limited use for image-like signals because they do not address directly the fundamental issues of how to quantify *shape* or *geometrical structure* in signals. In contrast, mathematical morphology, which is a set-theoretical methodology for image analysis, can rigorously quantify many aspects of the geometrical structure of signals in a way that agrees with human intuition and perception. This method, which has its mathematical origins in set theory, integral geometry, convex analysis, stereology, and geometrical probabilities, was developed mainly by Matheron [80], [81] and Serra [115] in the 1960s.

The techniques of mathematical morphology are based on set-theoretic concepts, on nonlinear superpositions of signals, and on a class of nonlinear systems that we call *morphological systems*. We consider the term mathematical morphology to be a more general designation, referring to the entire body of fundamental theory of morphological systems and to the heuristics and algorithms associated with application of the theory to specific areas. Mathematical morphology has been widely used for biomedical and electron microscopy image analysis, and it has been a valuable tool in many computer vision applications, especially in the area of automated visual inspection. Industrial applications of these techniques have been spurred by the continuous development and improvement of novel computer architectures for implementing morphological signal transformations. However, in spite of its many successful applications and its deep and elegant mathematical structure, mathematical morphology has only recently become a topic of interest for academic research, and the breadth and generality of the approach are not yet widely appreciated.

A comprehensive survey of the entire field of mathematical morphology would necessarily be very superficial even if much more space were available. Instead, we focus on morphological systems, with the goals of showing how these systems can enrich the mathematical tools of multidimensional signal processing and illustrating how they can be applied to fields of growing interest such as computer vision, nonlinear filtering, and structural signal analysis. Thus, we provide a review of the fundamentals of morphological system theory and we give an introduction to some of the elegant theorems that are available for representation and analysis of morphological systems. We also attempt to illustrate ways that morphological systems can be applied by showing a limited number of examples drawn primarily from our own past and current research [64]–[74]. While limited space precludes a detailed review of all previous work in the field of mathematical morphology, we have provided an extensive bibliography and have cited relevant contributions from other researchers wherever possible.

The paper is organized as follows. Section II reviews the basic concepts behind morphological systems. Section III contains applications to nonlinear filtering: relationships between morphological and rank-order/median filters, multiscale morphological smoothing, morphological sampling, and morphological correlation. Section IV covers some applications to image analysis: edge/blob feature extraction, shape representation via skeleton transforms, shape description via shape-size distributions, and descrip-

Manuscript received February 21, 1989; revised July 12, 1989. This work was supported in part by the National Science Foundation under Grant MIPS-86-58150, with matching funds from Bellcore, Xerox, and Sun, and by ARO under Grant DAAL03-86-K-0171, and by the Joint Services Electronics Program under Contract DAA03-87-K0059.

P. Maragos is with the Division of Applied Sciences, Harvard University, Cambridge, MA 02138, USA.

R. W. Schafer is with the School of Electrical Engineering, Georgia Institute of Technology, Atlanta, GA 30332, USA.

IEEE Log Number 9034605.

0018-9219/90/0400-0690$01.00 © 1990 IEEE

tion/modeling of fractal images. Section V shows that simple morphological operations are the representational prototypes of a large class of nonlinear and linear signal operators.

II. General Concepts

The basis for this approach to multidimensional signal processing is the representation of signals and systems in terms of sets and set transformations. This is the key to representing and manipulating geometric structure in images and other signals.

A. Signal Representations

Let **R** and **Z** denote, respectively, the set of real and integer numbers, and let **E** be the d-dimensional (henceforth denoted d-dim) continuous space $\mathbf{R}^d$ ($d = 1, 2, \cdots$) or the discrete space $\mathbf{Z}^d$. Then a d-dim signal can be represented as a function whose domain is either $\mathbf{R}^d$ (continuous) or $\mathbf{Z}^d$ (discrete), and whose range is either **R** (continuous amplitude) or **Z** (quantized amplitude).

Binary signals can be represented by sets. For example, the image at the top left of Fig. 1 is a binary signal, where the white background region could be represented by 0 and the shaded foreground could be represented by 1. Clearly the signal may also be represented by the set X of points corresponding to the shaded region. Binary images are often obtained by thresholding a gray-level image. Thresholding can also be used to represent gray-level images by binary signals and therefore, by sets. Serra [114], [115] uses the representation of a real-valued d-dim function $f(x)$ (x is a d-dim vector) by the ensemble of its d-dim *threshold sets* defined by

$$T_a(f) = \{x: f(x) \geq a\}, \qquad -\infty < a < \infty, \tag{1}$$

where the amplitude a spans all of **R** or **Z** depending on whether the signal f has a continuous or quantized range. The threshold sets have two important properties: They are

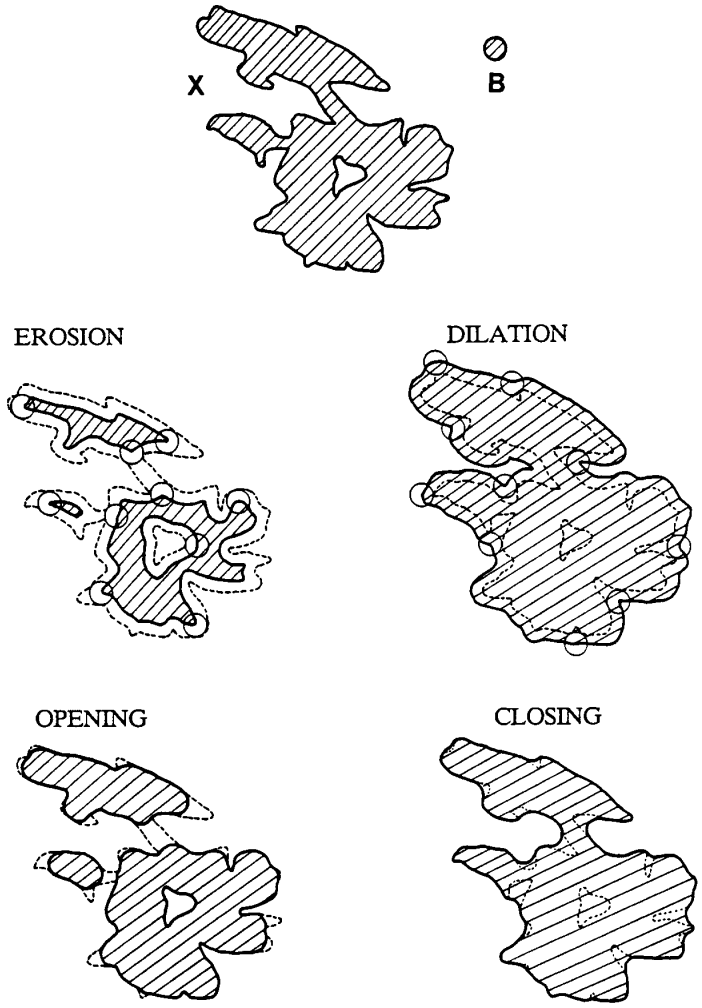

Fig. 1. Erosion, dilation, opening, and closing of X (binary image of an island) by a disk B centered at the origin. The shaded areas correspond to the interior of the sets, the dark solid curve to the boundary of the transformed sets, and the dashed curve to the boundary of the original set X. (From [73])

linearly ordered since $a < b \Rightarrow T_a(f) \supseteq T_b(f)$, and they can reconstruct the signal f uniquely since

$$f(x) = \max \{a: x \in T_a(f)\}, \quad \forall x. \tag{2}$$

This representation is illustrated for a 1-dim signal by the example of Table 1. The signal $f(x)$, shown in the second row of the table, has only four amplitude levels, and thus can be represented by the four threshold sets, each of which includes only the points indicated by dots in the next four rows of the table. (A continuous-amplitude signal would require an infinite number of threshold sets.) The final four rows show the *threshold binary signals* corresponding to the threshold sets where $f_a(x) = 1$ if $f(x) \geq a$ [i.e., $x \in T_a(f)$] and $f_a(x) = 0$ if $f(x) < a$ [i.e., $x \notin T_a(f)$], where a spans the range of $f(x)$. Obviously, the signals $f_a(x)$ convey the same information as the threshold sets $T_a(f)$. Hence, f can be reconstructed from the f_a's since

$$f(x) = \max \{a: f_a(x) = 1\}, \quad \forall x. \tag{3}$$

The validity of (2) and (3) is easily seen for the example of Table 1.

Table 1 Threshold Representation of a Discrete, Quantized Signal

x	0	1	2	3	4	5	6	7	8	9	10
$f(x)$	1	1	2	1	3	0	0	1	0	2	3
$T_3(f)$					•						•
$T_2(f)$			•		•					•	•
$T_1(f)$	•	•	•	•	•			•		•	•
$T_0(f)$	•	•	•	•	•	•	•	•	•	•	•
$f_3(x)$	0	0	0	0	1	0	0	0	0	0	1
$f_2(x)$	0	0	1	0	1	0	0	0	0	1	1
$f_1(x)$	1	1	1	1	1	0	0	1	0	1	1
$f_0(x)$	1	1	1	1	1	1	1	1	1	1	1

B. Signal Transformations

The signal transformations of mathematical morphology, which we call *morphological filters*,[1] are nonlinear signal operators that locally modify the geometrical features of multidimensional signals. We consider first the case of binary signals. Let $X \subseteq \mathbf{E}$ be the set representation of a binary input signal, and let $B \subseteq \mathbf{E}$ be a compact set of small size and simple shape (e.g. a d-dim ball). The set B is called a *structuring element*. Let $X \pm b = \{x \pm b: x \in X\}$ denote the vector *translate* of X by $\pm b \in \mathbf{E}$. The fundamental morphological operators for sets are *dilation* $\oplus$ and *erosion* $\ominus$ of X by B, which are defined as follows:

$$X \oplus B = \bigcup_{b \in B} X + b = \{x + b: x \in X \text{ and } b \in B\}, \tag{4}$$

$$X \ominus B = \bigcap_{b \in B} X - b = \{z: (B + z) \subseteq X\}. \tag{5}$$

From these definitions, it can be shown that the output of the dilation operator is the set of translation points such that the translate of the *reflected* structuring element $\check{B} = \{-b: b \in B\}$ has a nonempty intersection with the input set; i.e., $X \oplus B = \{z: (\check{B} + z) \cap X \neq \varnothing\}$. Similarly, the output of the erosion operator is the set of translation points such that the translated structuring element is contained in the input set.

Other operators can be defined as combinations of erosions and dilations. For example, two additional fundamental operators are *opening* $\circ$ and *closing* $\bullet$ of X by B defined as follows:

$$X \circ B = (X \ominus B) \oplus B, \tag{6}$$

$$X \bullet B = (X \oplus B) \ominus B. \tag{7}$$

To visualize the geometrical behavior of these operators it is helpful to consider 2-dim sets such as the set X and the structuring element B shown at the top of Fig. 1. Figure 1 shows that erosion shrinks the set X, whereas dilation expands X. The opening suppresses the sharp capes and cuts the narrow isthmuses of X, whereas the closing fills in the thin gulfs and small holes, in a way such that $X \circ B \subseteq X \subseteq X \bullet B$. Thus, if the structuring element B has a regular shape, both opening and closing can be thought of as nonlinear filters which smooth the contours of the input signal. Clearly, the shape and size of the structuring element will determine the nature and the degree of smoothing.

The above set operators can be extended to multilevel (i.e., non-binary) signals, represented by real-valued functions, in various ways [114], [115], [82], [89], [121], [122], [100]. Serra used the representation of a d-dim function $f(x)$ by the collection of its threshold sets in (1). Then, dilating all threshold sets of f by the same compact set B yields the sets $T_a(f) \oplus B$, which are the threshold sets of a new function $f \oplus B$, called the *dilation* of f by B. This new function can be computed either from (2) as $(f \oplus B)(x) = \max \{a: x \in T_a(f) \oplus B\}$ or, from the equivalent direct formula:

$$(f \oplus B)(x) = \max_{y \in B} \{f(x - y)\}. \tag{8}$$

Similarly, eroding all threshold sets of f by the same set B and superimposing all output sets via (2) yields a new function, the *erosion* of f by B, which can also be computed by the equivalent formula

$$(f \ominus B)(x) = \min_{y \in B} \{f(x + y)\}. \tag{9}$$

The *opening* $\circ$ and *closing* $\bullet$ of f by B are defined as $f \circ B = (f \ominus B) \oplus B$ and $f \bullet B = (f \oplus B) \ominus B$. The results of applying the erosion, dilation, opening and closing operations to the discrete quantized signal in Table 1 are given in Table 2 for the structuring set $B = \{-1, 0, 1\}$. Note that the endpoints of the outputs are undetermined because the shifts by the points of the symmetric structuring element require points outside the given domain [0, 10]. An alternative would be to assume some value for the signal outside the given interval. It is instructive to verify the results of Table 2 by using (8) and (9) and by applying the set-theoretic definitions to the threshold set representation of $f(x)$ in Table 1.

Table 2 Dilation, Erosion, Opening, and Closing of a Discrete, Quantized Signal

x	0	1	2	3	4	5	6	7	8	9	10
$f(x)$	1	1	2	1	3	0	0	1	0	2	3
$f(x) \oplus B$	-	2	2	3	3	3	1	1	2	3	-
$f(x) \ominus B$	-	1	1	1	0	0	0	0	0	0	-
$f(x) \circ B$	-	-	1	1	1	0	0	0	0	-	-
$f(x) \bullet B$	-	-	2	2	3	1	1	1	1	-	-

[1] In [56], [116] the term "morphological filters" refers only to a special class of morphological transformations (algebraic generalizations of openings), whereas we use it interchangeably with the broader term *morphological systems*.

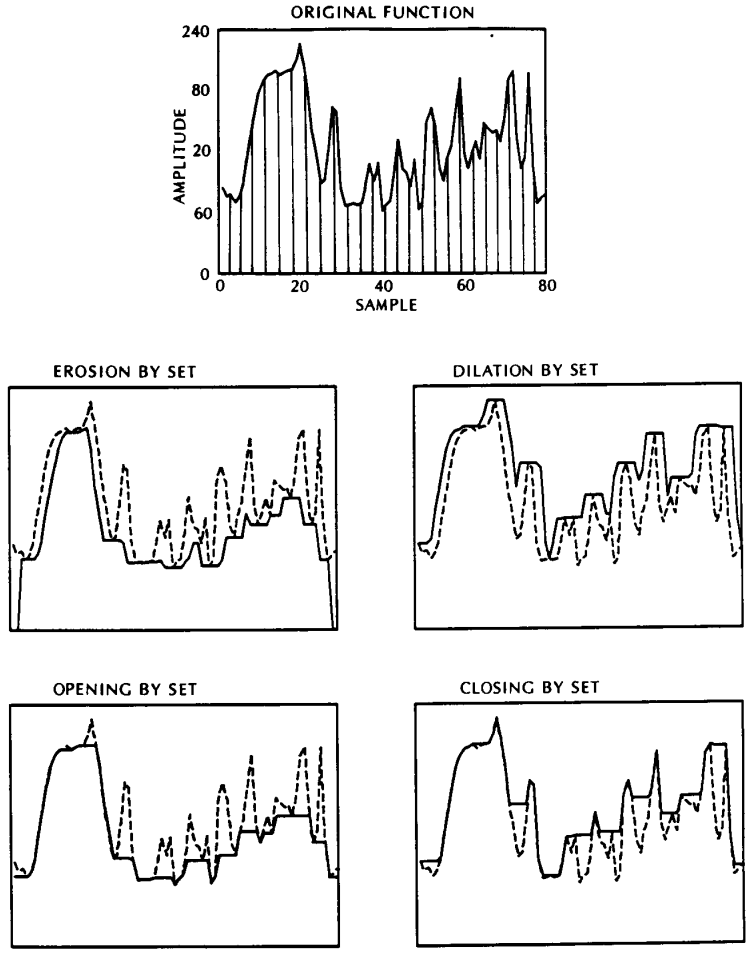

Fig. 2. Erosion, dilation, opening, and closing of a 1-dim discrete signal of 80 samples by a 1-dim set $B = \{-2, -1, 0, 1, 2\}$. The shaded region is the umbra of the input signal, and the dashed curves in the lower four plots are the input signal. (From [73])

Figure 2 shows another set of results of applying the basic morphological operators to a 1-dim signal. In Fig. 2 we see that erosion of a function f by a small convex set B reduces the peaks and enlarges the minima of the function. The dilation of f by B increases the valleys and enlarges the maxima of the function. The opening by B smoothes the graph of f from below by cutting down its peaks, and the closing smoothes the graph of f from above by filling up its valleys. Clearly, a larger 1-dim structuring set would have a greater smoothing effect.

Another extension of morphological operators to functions is due to Sternberg [121], [122], who uses the representation of a d-dim function $f(x)$ by a $(d + 1)$-dim set, its *umbra*

$$U(f) = \{(x, a): a \leq f(x)\}; \tag{10}$$

i.e., the umbra is the set of points *below* the surface represented by $f(x)$. In Fig. 2, the umbra of $f(x)$ is the shaded region. Likewise, the umbrae of the outputs of the erosion, dilation, opening, and closing would be the regions below the solid curves in respective plots in Fig. 2. In general, the umbra set extends to $a = -\infty$. The function can be reconstructed from its umbra since

$$f(x) = \max \{a: (x, a) \in U(f)\}, \qquad \forall x. \tag{11}$$

Dilating or eroding the umbra of f by the umbra of g yields the umbrae of new functions, i.e., the dilation or erosion of f by g. These two new functions can be computed from the direct formulae:

$$(f \oplus g)(x) = \max_y \{ f(y) + g(x - y)\} \tag{12}$$

$$(f \ominus g)(x) = \min_y \{ f(y) - g(y - x)\} \tag{13}$$

where for each x, y ranges over the intersection of the "support" of f and the (shifted by x) support of g. By *support* of f here we mean the set of x at which $f(x) \neq -\infty$.[2] The function g is assumed to possess a compact support and plays the role of a structuring element. The opening and closing

[2]For max/min operations, $-\infty$ plays a similar role to that played by 0 for additions/multiplications. Thus, to define morphological operators on functions it helps to set their values outside their supports as equal to $-\infty$.

of f by g are, respectively, the functions $f \circ g = (f \ominus g) \oplus g$ and $f \bullet g = (f \oplus g) \ominus g$.

In this paper we have presented the various theoretical concepts in a way that emphasizes intelligibility at the expense of absolute mathematical correctness. Thus, the mathematically inclined reader may find fault with some of the above definitions. For example, some of the above max/min operations may have to be replaced by sup/inf, and the assumption about real-valued signals may have to be supplemented by also allowing the signals to assume $\pm\infty$ values. Note that, for signals that assume the extreme values $\pm\infty$, the maximum in (2), (3) and (11) must be replaced with supremum. A more rigorous treatment of the morphological operators and their properties can be found in [28], [43], [47], [68], [73], [110], [115].

In [116, ch. 1, 2] Serra has extended the morphological operators to more abstract spaces such as *lattices*. Serra's lattice framework has been further investigated by Heijmans and Ronse [47], [110]. Whereas all the morphological operators discussed in this paper are translation-invariant, in [109] dilations and erosions on the Euclidean plane are considered that are invariant under rotation and scalar multiplication.

C. Historical Notes

Considerable confusion has arisen regarding the definitions of the basic operations of mathematical morphology. This confusion is primarily due to usage of the symbols $\oplus$ and $\ominus$ by different authors to mean different things. The Appendix gives a discussion of the different definitions and shows how they are related.

Parallel to the evolution of the morphological operations that we have discussed, many other researchers studied image processing techniques based on cellular array computers and similar operations of the shrink/expand type. Early papers include [40], [53], [86], [99], [113], [133]. Recent surveys of such approaches can be found in [101], [112]. Most of these efforts dealt with binary images. The extension to gray-level images was done by using concepts from fuzzy set theory [52], [142]. Nakagawa and Rosenfeld [89] introduced the local min/max operators on digital gray-level images as an extension of the shrink/expand operators on binary images. Goetcherian [39] extended many binary image processing algorithms to gray-level images. Preston [100] used an umbra-like approach to extend the morphological operators to gray-level signals by operating on binary representations of the signals' umbrae with threshold logic operators. All these related contributions can be formalized under the rich theoretical framework of mathematical morphology, as we outline in this paper.

D. Nonlinear Superpositions

Linear operators commute with additive superposition (i.e., pointwise addition) of signals. Morphological operators commute with some nonlinear signal superpositions, which are induced by set operations (unions/intersections) among the threshold sets or umbrae of two signals f and g. Specifically, for all a, it is easily shown that $T_a(f \wedge g) = T_a(f) \cap T_a(g)$ and $T_a(f \vee g) = T_a(f) \cup T_a(g)$, where the operations $\wedge$ and $\vee$ are defined by $(f \wedge g)(x) = \min\{f(x), g(x)\}$ and $(f \vee g)(x) = \max\{f(x), g(x)\}$. Likewise, the umbrae of $f \wedge g$ and $f \vee g$ are, respectively, the intersection and union of $U(f)$ and $U(g)$. Therefore dilation commutes with $\vee$ and erosion commutes with $\wedge$:

$$(f \vee g) \oplus h = (f \oplus h) \vee (g \oplus h)$$
$$(f \wedge g) \ominus h = (f \ominus h) \wedge (g \ominus h) \quad (14)$$

These results can be generalized for an infinite number of signals by using $\wedge$ and $\vee$ to generally denote pointwise infimum and supremum.

Parallel superposition of morphological operators is possible by using the nonlinear signal combinations of pointwise max/min. Specifically, let $\Psi_1(f)$ and $\Psi_2(f)$ be the output signals from two morphological operators when the input is f. Then, the operator $\Psi_{max}(f) = \Psi_1(f) \vee \Psi_2(f)$ is the max-superposition of the operators Ψ_1 and Ψ_2. We can also define the min-superposition operator $\Psi_{min}(f) = \Psi_1(f) \wedge \Psi_2(f)$. For morphological set operators these parallel superpositions still apply if we replace pointwise max/min of signals with union/intersection of sets. Finally, two morphological operators can be *cascaded* by applying one of the operators to the output of the other; e.g., the opening is the cascade of an erosion and a dilation.

A helpful *classification* of morphological operators results by focusing on a specific characteristic of the input/output signals: whether they are binary (sets) or multilevel (functions). We call the operators of (12) and (13) and their cascade or parallel (using $\wedge$, $\vee$) combinations *function-processing* (*FP*) operators, because they accept as inputs d-dim functions and produce as outputs d-dim functions. Likewise, the morphological set operators (4)–(7) and their cascade or parallel (using $\cap$, $\cup$) combinations are *set-processing* (*SP*) operators. A subclass of FP operators are called *function- and set-processing* (*FSP*) because they can process d-dim binary signals without changing this (binary) signal characteristic; thus FSP operators can switch between two modes of operations, FP or SP. Examples of FSP operators are the FSP dilation and erosion of f by B in (8) and (9); these are special cases of the FP dilation and erosion of f by g in (12), (13) if B is equal to the support of g, and g is equal to 0 inside B and $-\infty$ outside B.

E. Implementations

The evolution of the theory of mathematical morphology has closely followed the evolution of many generations of novel (pipelined or parallel) computer architectures designed to implement morphological operations. Most of these architectures were developed as cellular automata machines to extract pictorial information. Early examples include [31], [54], [61], [120]. For relative comparisons see [23]. More recent architectures can be found in [49], [50], [77], [144], [145] and in the long list of papers on morphological systems presented in [102].

The scope of this paper does not permit explaining any of these architectures in any length. Instead we briefly discuss a *parallel* implementation of binary erosions and dilations [120] to illustrate some major issues. As (4) and (5) imply, a *global* approach to obtaining the dilation or erosion, respectively, of a binary image X by a structuring element B is to take the union or intersection of translates of X by vector points in B. Figure 3 shows an implementation of this idea, where two bit planes are needed to hold X and B and a third accumulator bit plane for the resulting transformed image. The image plane is shifted in parallel to the

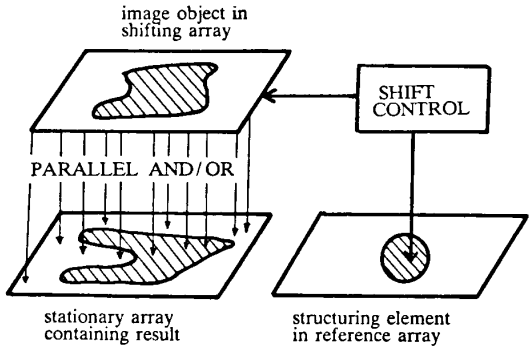

Fig. 3. Parallel implementation of binary erosion and dilation. (Adapted from [120])

accumulator plane, and the amount of shifting is controlled by the points belonging to the structuring element. The accumulator holds the parallel Boolean OR or AND of all the shifted versions of the image plane, and after all the points of B have been spanned, it will contain the dilation or erosion, respectively, of X. Alternatively, a *local* approach to compute the erosion and dilation is to shift the window B everywhere in the image plane and simultaneously perform local neighborhood operations of the Boolean type. The efficiency and scope of these simple implementations can be greatly enriched by using the rich set of algebraic properties of morphological operators. They can also be extended to gray-level images by using either max/min operations or threshold superposition (see Section II-B).

III. Applications to Nonlinear Filtering

Morphological systems, composed (at their lowest level) of erosions and dilations, can be used to modify multidimensional signals in ways that are analogous to linear filtering. The definitions of erosion and dilation indicate that these operations are similar in complexity to convolution with a finite[3] duration impulse response in the sense that the output at a given point is dependent on input values in a neighborhood of that point. However, morphological filters are nonlinear and have distinctly different properties and capabilities from linear filters. In this section we consider several types of morphological and related nonlinear filters.

A. Rank-Order and FSP Morphological Operators

Median filters and, their generalization, *rank-order filters* are nonlinear discrete[4] operators that have become popular for smoothing and enhancement of image and other signals. (See [2], [12], [17], [38], [51], [58], [91], [127], [129], for various properties and applications.) In this section, we review from [74] some interesting interrelationships among rank-order and FSP morphological operators.

The similarity between morphological filters and rank-order filters is illustrated by Fig. 4. Median filters are attractive for removing impulsive (or salt-and-pepper) noise in images since they can remove the noise without blurring edges as would be the case for linear filtering. Figure 4 shows that in this application, the median behaves like a combined opening and closing, i.e., an open-closing $(f \circ B) \bullet B$, by a set B of size about half the size of the median window. In addition, the open-closing, while requiring less computation than the median, decomposes the noise suppression task into two steps; i.e., the opening suppresses the positive noise impulses, and the closing suppresses the negative noise impulses. The median filter does not discriminate between positive and negative impulses.

Let $W \subseteq \mathbf{Z}^d$ be a finite set called the *window* of the rank-order filter. Assume that $|W| = n$ points, where $|\cdot|$ denotes set cardinality. For $r = 1, 2, \cdots, n$, the output $RO_r(f; W)(x)$ of the rth rank-order filter with window W is obtained at any location $x \in \mathbf{Z}^d$ by *sorting* into descending order the n values of the input function f inside the shifted window $W + x$ and picking the rth number from the sorted list. If n is odd and $r = (n + 1)/2$ we have the special case of the median filter $med(f; W)$ of f with window W. Rank-order filters are FSP operators. To define their corresponding SP operators consider discrete input sets $X \subseteq \mathbf{Z}^d$. The rth SP rank-order filter is the set operator whose output is

$$RO_r(X; W) = \{p: |X \cap (W + p)| \geq r\}. \tag{15}$$

Note that computing the output from an SP rank-order filter involves only *counting* of points and no sorting. Thus, an equivalent way to implement the binary rank-order filters is to linearly convolve the binary input signal with a binary impulse response whose domain is W and then threshold the result at a level corresponding to the rank r.

The theoretical analysis of these useful filters is difficult because they are nonlinear and have nonzero memory. However, by using mathematical morphology, the framework presented in [74] facilitates the theoretical analysis of these filters, relates them to morphological filters, and provides some new realizations for them. Specifically, from the definition it is clear that the last rank-order filter ($r = n$) is identical to the erosion by W. Likewise, the first rank-order filter ($r = 1$) with window W is identical to the FSP or SP dilation by $\check{W}$. Further, all rank-order filters commute with thresholding [36], [51], [74], [89], [115], [130]; i.e.,

$$T_a[RO_r(f; W)] = RO_r[T_a(f); W], \qquad \forall a. \tag{16}$$

This property is also shared by many FSP morphological operators. Further, if we combine it with (2), it implies that, if Ψ is any FSP operator commuting with thresholding, then

$$[\Psi(f)](x) = \max\{a: x \in \Psi[T_a(f)]\} \qquad \forall x. \tag{17}$$

Therefore, as developed in [115] and [74], to transform a multilevel signal f by Ψ is equivalent to decomposing f into all its threshold sets, transforming each set by the binary counterpart of Ψ, and reconstructing the output signal $\Psi(f)$ via the threshold-max superposition of (17). This allows us to study all rank-order filters (which include erosion and dilation) and their cascade (e.g., opening and closing) or parallel (using $\vee$, $\wedge$) combinations by focusing on their corresponding binary filters. Such representations are much simpler to analyze and they suggest alternative implementations that do not involve numeric comparisons or sorting.

Using this approach, many interesting and useful relationships between rank-order filters and morphological fil-

[3]The computational structure of all the morphological and rank-order filters examined in this paper is similar to that of *non-recursive* linear filters. *Recursive* erosions and dilations have been used in [9], [112], [113] for fast computations of distance transforms. Recursive rank-order filters are defined in [91].

[4]For *analog* rank-order filters see [37], [60].

Fig. 4. (a) A 256 × 256-pixel (8-bit/pixel) gray-level image f corrupted with salt-and-pepper noise; SNR = 15.1 dB. (Probability of occurrence of noisy samples is 0.1.) (b) Opening $f \circ B$ of f by a 2 × 2-pixel square set B; SNR = 19.5 dB. (c) Open-closing $(f \circ B) \bullet B$; SNR = 25.8 dB. (d) Median of f by a 3 × 3-pixel window; SNR = 29.1 dB. The SNRs were computed by 20 $\log_{10}(255/e_{rms})$, where e_{rms} was the rms-value of the difference between the original and the noisy or restored images. (From [74])

ters were obtained in [74]. For example, it was shown that any rank-order filter can be represented as either a max-superposition of erosions or a min-superposition of dilations. Such implementations avoid sorting and require a fixed computation to compute each output sample. Reference [74] also presents a number of properties of median root signals and relations between median roots and close-openings and open-closings.

B. Threshold Superposition and Stack Filters

In Section II-A we showed that a function $f(x)$ can be represented exactly by the set of its threshold binary signals $f_a(x)$. If f is *nonnegative* and, say for simplicity, has integer uniformly spaced amplitudes $a = 0, 1, 2 \cdots$, then f can also be reconstructed as the pointwise sum of the f_a's; i.e.,

$$f(x) = \sum_{a \geq 1} f_a(x) \tag{18}$$

Fitch *et al.* [36] showed that for nonnegative digital signals f, rank-order operators Ψ obey a *threshold-sum superposition* of the form:

$$\Psi(f) = \sum_a \Psi(f_a). \tag{19}$$

This weak form of linear superposition holds because the f_a's are binary and linearly ordered; i.e., $a < b \Rightarrow f_a \geq f_b$. Note that (19) is a special case of (17) since the former applies only to nonnegative signals. Both types of threshold superposition for rank-order filters have proved to be important for VLSI [46] and optical-electronic implementations [49], [92].

Serra's general approach [114], [115, ch. XII] of creating a multilevel signal operator $f \mapsto \Psi(f)$ from a binary operator $X \mapsto \Psi(X)$ requires that Ψ has two properties: it must be *increasing* [$X \subseteq Y \Rightarrow \Psi(X) \subseteq \Psi(Y)$] and it must be *upper semicontinuous* [for any decreasing set sequence (X_n) with $X_{n+1} \subseteq X_n$, $\Psi(\cap_n X_n) = \cap_n \Psi(X_n)$.] If these conditions hold for an arbitrary SP operator Ψ, then the $\Psi[T_a(f)]$ are legitimate threshold sets of an output function $\Psi(f)$ synthesized via (17); hence, an FSP operator is created. In [74] we applied (17) to rank-order and FSP morphological operators.

Wendt *et al.* [134] defined *stack* filters by using similar concepts as in [115] and [74], but from a different viewpoint, and their result was applicable only to discrete filters. In their work, the role of the set operator Ψ was played by a *positive Boolean function* β, which, due to its monotonicity, is increasing [88]. The "increasing" property is called "stacking" in [134]. Further, by filtering all threshold binary signals f_a with β and using the threshold-sum superposition (19), they defined a stack filter ST_β as

$$ST_\beta(f) = \sum_a \beta(f_a). \tag{20}$$

In [74] we showed that all stack filters are finite pointwise maxima or minima of moving local min/max operators, and vice-versa.

All the previous discussion about threshold superposition referred to FSP operators. Serra [115, p. 444] obtained

analogous results for FP dilations and erosions. Similar decompositions of gray-level dilations into multiple binary dilations have been developed in [117] for VLSI architectures.

C. Multiscale Nonlinear Smoothing

In computer vision research [78] it has become apparent that various image analysis tasks have to be performed not at a single image scale but at multiple scales, because image features occur on a variety of scales. One approach to quantifying scale [16], [79], [111], [137], [140] involves varying the average "width" σ of the impulse response (e.g., a Gaussian) of a linear low-pass filter that smoothes the image. Despite the mathematical tractability of this linear filtering approach, linear filters shift and blur important image features such as edges. Alternatively, there is a large class of *nonlinear* filters including median and opening/closing filters that avoid this problem, because they can provide signal smoothing by eliminating impulses or narrow peaks/valleys while preserving its edges. In [65], [66], [69] Maragos investigated an approach for multiscale nonlinear image smoothing based on openings and closings. Some of the reasons for focusing on openings/closings are the following:

1. As developed in Matheron [81], openings and closings of sets in Euclidean spaces by convex sets of varying size (scale) can formalize the concept of size.
2. A new definition of scale is possible based on openings. Specifically, let $B \subseteq \mathbf{Z}^2$ be a finite connected set. If B is of size (by convention) one, the sets

$$nB = \underbrace{B \oplus B \oplus \cdots \oplus B}_{n\text{times}} \tag{21}$$

define binary structuring elements of discrete size $n = 0, 1, 2, \cdots$. If B is convex, then nB is shaped like B but has size n. The *multiscale opening* of a binary image X by B at scale $n = 0, 1, 2, \cdots$ is defined [69] by

$$X \circ nB = [(X \underbrace{\ominus B) \ominus B \cdots \ominus B}_{n\text{times}}] \underbrace{\oplus B \oplus B \cdots \oplus B}_{n\text{times}}. \tag{22}$$

A *dual* multiscale filter is the closing $X \bullet nB = (X \oplus nB) \ominus nB$. If $n = 0$, then $nB = \{0\}$, the origin point, and $X \circ nB = X \bullet nB = X$. The opening $X \circ nB$ eliminates from X all objects of size $< n$ (with respect to B), that is, objects inside which nB cannot fit, because, as can be shown,

$$X \circ nB = \bigcup_{(nB+z) \subseteq X} (nB + z). \tag{23}$$

That is why, the size n of nB can be considered to be synonymous to the scale at which the filter $X \circ nB$ operates. Equation (23) implies that scale could be defined as the smallest size n of a prototype pattern B that can fit inside the image X. This definition of scale is more rigorous than the approximate definition in linear smoothing.
3. An important property of the multiscale Gaussian filters for edge detection is that they do not introduce additional zero-crossings as the scale (σ) increases. Chen and Yan [18] have proved something similar for the multiscale openings; specifically, they showed that openings of 1-D boundary curvature functions of continuous binary images by disks do not introduce additional zero-crossings at coarser scales (larger disk radii).
4. Finally, Brockett [14] found a nonlinear partial differential equation that models the continuous multiscale FSP openings as a dynamical system.

The multiscale openings can be extended [69] to gray-level images $f(x)$, $x \in \mathbf{Z}^2$, as follows. Let $g(x)$ be a gray-level structuring function-element, with a finite connected support of size one. Then

$$ng = \underbrace{g \oplus g \oplus \cdots \oplus g}_{n\text{times}} \tag{24}$$

defines structuring functions of size $n = 0, 1, 2, \cdots$. The *multiscale opening* of f by g at scale $n = 0, 1, 2, \cdots$ is defined as

$$f \circ ng = [(f \underbrace{\ominus g) \ominus g \cdots \ominus g]}_{n\text{times}} \underbrace{\oplus g \oplus g \cdots \oplus g}_{n\text{times}} \tag{25}$$

Likewise, $f \bullet ng = (f \oplus ng) \ominus ng$ is the *multiscale closing* of f by g. See Fig. 5 for examples.

If the image contains 1-dim line structures to be preserved, then the opening by ng will eliminate them if g has a 2-dim support. This can be avoided by using a max-superposition of openings or closings by 1-dim structuring elements oriented at various angles. Thus, for preserving edge/line features that have a predominant 1-dim structure the following multiscale morphological smoothing operators can be used:

$$[O_n(f)](x) = \max_{\theta} \{ f \circ ng_\theta(x) \} \tag{26}$$

$$[C_n(f)](x) = \min_{\theta} \{ f \bullet g_\theta(x) \}, \tag{27}$$

where g_θ is a 1-dim structuring element (binary or gray-level) rotated at angle θ. For digital implementations θ spans only a finite set of different orientations, e.g., 0°, 45°, 90°, 135°.) Applications of these parallel superpositions of oriented openings can be found in [69], [104], [115], [116], [124].

D. Morphological Sampling

Digitalization of continuous binary images by sampling them on periodic grids causes some loss of information. The issue of which morphological operators are "digitalizable," i.e., satisfy a continuity condition in the transition from the continuous to discrete domain was analyzed in [115]. The errors of derived measurements were examined in [29].

Another aspect of sampling involves multiresolution techniques [16], [111], [128], which have proven to be very useful in computer vision. Creating a multiresolution pyramid requires multiple steps of smoothing the image and sub-sampling it. Such concepts are very similar to the ones encountered in classical signal decimation/interpolation [93]. Most research in image pyramids has been based on linear smoothers. However, since morphological filters preserve essential shape features, they may be superior in many applications. Further research is required to dem-

Fig. 5. Multiscale openings and closings. (a) Graytone image f (256 × 256 pixels). (b) $f \circ ng$, $n = 1, 2, 3$ (top to bottom). The pattern g is defined on $\mathbf{Z}$ as $g(x, y) = 5\sqrt{5 - x^2 - y^2}$, $0 \le x^2 + y^2 \le 5$, and $g(x, y) = -\infty$ if $x^2 + y^2 > 5$. (c) $f \circ ng$, $n = 4, 5, 6$ (top to bottom). (d) $f \bullet ng$, $n = 1, 2, 3$ (top to bottom). (e) $f \bullet ng$, $n = 4, 5, 6$ (top to bottom). (From [69])

onstrate the utility of morphological filters in forming multiresolution imagery.

Haralick, Lin, Lee and Zhuang [44], [45] have addressed some of these issues and developed a theory of morphological sampling. Their work provides a number of interesting results on reconstructing a signal after morphological smoothing and decimation. For example, they showed that if a binary signal represented by a set F has been smoothed first to $X = F \circ K$ by opening it with a structuring element K and then down-sampled to $X \cap S$ by intersecting it with a periodic sampling set S [S and K must satisfy certain conditions], then the Hausdorff distance between the smoothed signal X and its reconstruction $(X \cap S) \oplus K$ via dilation does not exceed the radius of K. By representing functions by umbrae, they have also extended these results to multilevel signals.

E. Morphological Correlation

Consider two real-valued d-dim discrete signals $f(n)$ and $g(n)$. Assume that g is a signal pattern to be found in f. To find which shifted version of g "best" matches f a standard approach has been to search for the shift lag k that minimizes the *mean squared error* $E_2(k) = \Sigma_{n \in W}[f(n + k) - g(n)]^2$ over some subset W of $\mathbf{Z}^d$. Under certain assumptions, this matching criterion is equivalent to maximizing the *linear cross-correlation* $\gamma(k) = \Sigma_{n \in W} f(n + k)g(n)$ between f and g. Such ideas have provided the foundations for many decades of research in matched filtering and signal detection. Although less mathematical tractable than the mean squared error criterion, a statistically more robust criterion is to minimize the *mean absolute error*

$$E_1(k) = \sum_{n \in W} |f(n + k) - g(n)|.$$

Mean absolute error criteria have been applied to template matching problems in image/signal processing and recently [20] to solving optimization problems in rank-order filtering.

In [67] Maragos linked the mean absolute error criterion with a nonlinear signal correlation used for signal matching. Specifically, since $|a - b| = a + b - 2\min(a, b)$, under certain assumptions (e.g., if the error norm and the correlation is normalized by dividing it with the average area under the signals f and g), minimizing $E_1(k)$ is equivalent to maximizing the *nonlinear* cross-correlation

$$\mu(k) = \sum_{n \in W} \min[f(n + k), g(n)].$$

It was shown experimentally and theoretically that the detection of g in f is indicated by a sharper matching peak in $\mu(k)$ than in $\gamma(k)$. This is illustrated in Fig. 6. In addition, the nonlinear correlation μ (a sum of minima) is often faster than the linear (sum of products) correlation γ. These two advantages of the nonlinear correlation coupled with the relative robustness of the mean absolute error criterion make μ promising for general signal matching.

IV. Applications to Image Analysis

The applications of morphological filters in image processing and analysis are numerous. Next we shall review some of these applications to specific problems in feature extraction, shape representation and description. Additional areas of applications (not further elaborated in this paper) include biomedical image processing [1], [19], [83], [108], [115], [118], [121]; geological image processing [34]; automated industrial inspection [24], [63], [123], [138]; shape recognition [21]; shape smoothing [69], [115], [126]; enhancement and noise suppression [39], [115], [112]; texture analysis [115], [135]; radar object detection [125]; and range imagery [33].

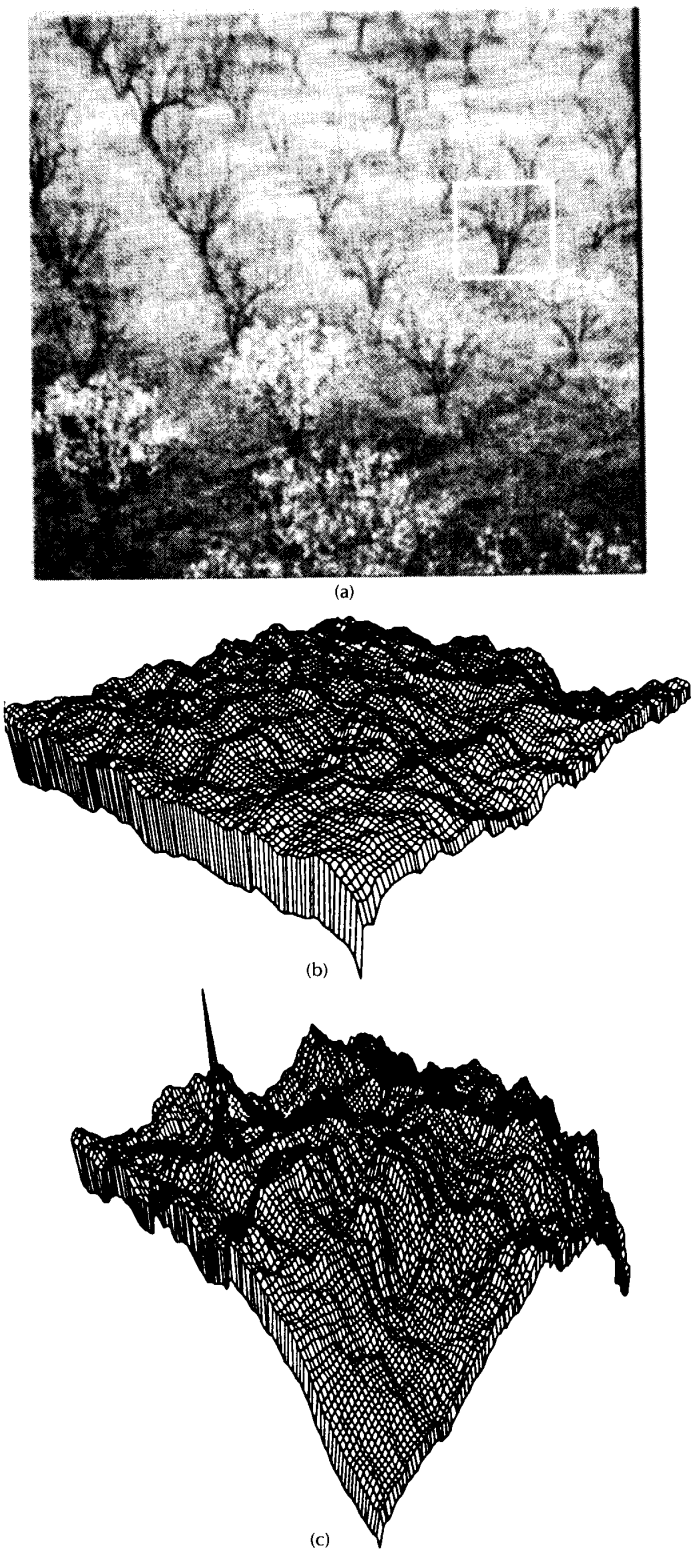

Fig. 6. (a) An image signal f (digitized from A. Adams' "Orchard") and a template g inside the window. (b) Linear correlation γ normalized by dividing it by the product of the rms value of g and the local rms value of f. (c) Morphological correlation μ normalized by dividing it by the average of the area under g and the local area under f. (From [67])

A. Feature Extraction

1) Edge/Line Enhancement and Detection: If W is a small 2-dim symmetric binary structuring element, then the set difference $X \setminus (X \ominus W)$ gives the boundary of a binary image X, and the algebraic difference

$$EG(f) = f - (f \ominus W), \tag{28}$$

which we may call an *erosion gradient*, enhances the edges of a gray-level image f [39], [71], [82], [115]. A similar edge-enhancing operator is the *dilation gradient*

$$DG(f) = (f \oplus W) - f. \tag{29}$$

By combining the two operators, new edge operators can be obtained that treat more symmetrically the image and its background. Examples include: 1) Beucher's morphological gradient $EG(f) + DG(f)$ in [115, p. 441] (see Fig. 7 for an example); 2) the morphological edge-strength operators $\min[EG(f), DG(f)]$ and $\max[EG(f), DG(f)]$ by Lee *et al.* [57]; and 3) the nonlinear Laplace operator $DG(f) - EG(f)$ in [131].

These morphological edge operators can be made more robust for edge detection by first smoothing the input image signal f either with a linear blur [57] or with an alpha-trimmed filter [35]. Another approach [131] involves combining the nonlinear Laplace filter for zero-crossing with the morphological edge-strength operators. As thoroughly investigated in [57], [131], these hybrid edge detection schemes, largely based on morphological gradients, perform comparably and in some cases better than several conventional schemes based only on linear gradients/filters; further, the morphological gradients are computationally more efficient.

In [76] it was shown that the edge operators $EG(f)$ and $DG(f)$ obey a threshold-sum superposition:

$$EG(f) = \sum_a EG(f_a). \tag{30}$$

Thus the gray-level edge operator $EG(f)$ can be analyzed and implemented by focusing on the much simpler binary edge operator $EG(f_a) = f_a - (f_a \ominus W)$ applied to the threshold binary images f_a.

2) Peak, Valley, and Blob Detection: Opening and closings offer an intuitively simple and mathematically formal way for peak or valley detection. As suggested by the example of Fig. 2 subtracting the opening of a signal f by a set B from the input signal yields an output consisting of the

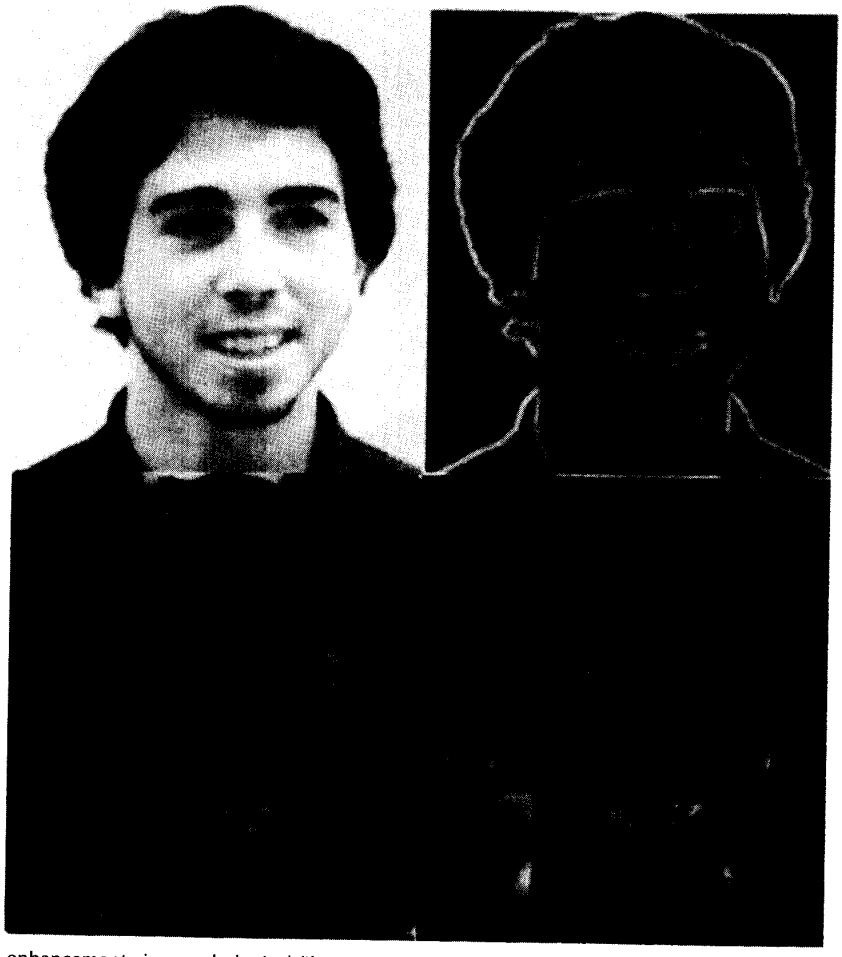

Fig. 7. Facial feature enhancement via morphological filtering. Top left: original 300 × 260-pixel image f. Top right: Edges $(f \oplus B) - (f \ominus B)$, where B is a 21-pixel discrete octagon. Bottom left: Peaks $f - (f \circ 3B)$. Bottom right: Valleys $(f \bullet 3B) - f$.

signal peaks whose support cannot contain B. This is Meyer's *top-hat transformation* [82], [83], [115],

$$P(f) = f - (f \circ B). \tag{31}$$

Since $f \circ B \leq f$, $P(f)$ is always a nonnegative signal, which guarantees that it contains only peaks. If the objective is to detect a *blob*, defined as a region with significantly brighter intensities relative to the surroundings, then we can identify the blob as a binary shape, a set B, which is the support of a corresponding peak in the intensity image function. The shape of the peak's support obtained by (31) is controlled by the shape of B, whereas the scale of the peak is controlled by the size of B. An example of application of the top-hat transformation is given in [104].

Similarly, if the blob to be detected occurs as an intensity valley, then we can approach the problem of blob detection by detecting a valley in f with a spatial support shaped like B. Thus, the operator

$$V(f) = (f \bullet B) - f \tag{32}$$

works as a general *valley* generating process. The ability of the morphological gradients to enhance edges and of the opening or closing residues to extract peaks or valleys is illustrated in Fig. 7. An example of applying these operators can be found in [141] as a pre-processing stage for extracting features such as eyes and mouth from images of human faces. Noble [90] has analyzed similar morphological feature detectors from the viewpoint of differential geometry.

In the computer vision literature there are also curvature-based approaches to extract peaks and valleys. The morphological peak/valley extractors, in addition to their being simple and efficient, have the following advantages [139] over the curvature-based approaches: 1) Curvature is an intrinsic property of 3-dim objects, which should remain invariant after 3-dim rotations. However, image functions cannot be arbitrarily rotated. Hence, the curvature estimates derived on functions are biased. 2) Using the curvature extrema to find the peak/valley boundaries may give results that do not agree with the visual perception of these boundaries. 3) Curvature requires 2nd-order derivatives, which amplify noise and are not well defined on discrete signals.

B. Shape Representation

Since the *medial axis transform* (also known as symmetric axis or skeleton transform) was first introduced by Blum [7], [8], it has been studied extensively for shape representation and description, which are very important issues in computer vision. A survey on skeletonization can be found in [112]. Next we explain how such transformations can be represented in terms of morphological systems.

Binary Images: Among the many approaches (i.e., via distance transforms [113]) to obtain the medial axis transform, it can also be obtained via erosions and openings [55], [72], [87], [115]. Let $X \subseteq \mathbf{Z}^2$ represent a finite discrete binary image and let $B \subseteq \mathbf{Z}^2$ be a binary structuring element containing the origin. The nth *skeleton component* of X with respect to B is the set

$$S_n = (X \ominus nB) \setminus [(X \ominus nB) \circ B], \qquad n = 0, 1, \ldots, N, \tag{33}$$

where $N = \max\{n: X \ominus nB \neq \varnothing\}$ and $\setminus$ denotes set difference. The S_n are disjoint subsets of X, whose union is the *morphological skeleton* of X. We define the *morphological skeleton transform* of X to be the finite sequence $(S_0, S_1, \cdots, S_N)$. From this sequence we can reconstruct openings of X; i.e.,

$$X \circ kB = \bigcup_{k \leq n \leq N} S_n \oplus nB, \qquad 0 \leq k \leq N. \tag{34}$$

Thus, if $k = 0$ (i.e., if we use all the skeleton subsets), $X \circ kB = X$ and we have *exact reconstruction*. If $1 \leq k \leq N$, we obtain a *partial reconstruction*, i.e., the opening (smoothed version) of X by kB. The larger the size index k, the larger the degree of smoothing. Figure 8 shows a detailed description of the skeletal decomposition and reconstruction of an image. Note that by varying k in the reconstruction phase, multiscale smoothed versions of X (its openings) can be obtained. Thus, we can view the S_n as "*shape components.*" That is, skeleton components of small size indices n are associated with the lack of smoothness of the boundary of X, whereas skeleton components of large indices n are related to the bulky interior parts of X that are shaped similarly to nB.

A variety of skeletons results from varying the structuring element, consistent with the ability of morphological sys-

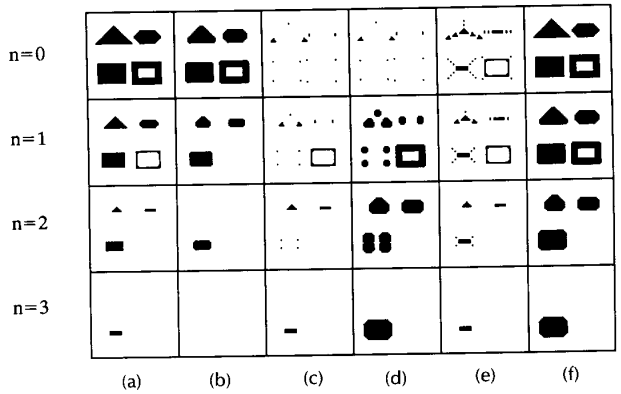

Fig. 8. Morphological skeletonization of a binary image X (top left image) with respect to a 21-pixel octagon structuring element B. (a) Erosions $X \ominus nB$, $n = 0, 1, 2, 3$. (b) Openings of erosions $(X \ominus nB) \circ B$. (c) Skeleton subsets S_n. (d) Dilated skeleton subsets $S_n \oplus nB$. (e) Partial unions of skeleton subsets $\cup_{N \geq k \geq n} S_k$. (f) Partial unions of dilated skeleton subsets $\cup_{N \geq k \geq n} S_k \oplus kB$. (From [72])

tems to extract different structural information by using different structuring elements. One application for producing multiple skeletons each with respect to a different structuring element was described in [72], where searching for the element that gives the skeleton with fewest points yielded the lowest information rate required to encode the image from its skeleton.

The morphological skeleton may be redundant. Thus, at the expense of producing a skeleton that may not look like a skeletal axis, we define the *minimal skeleton* to be a proper subset of the original skeleton whose points are sufficient for exact reconstruction, but removal of just one point would result in partial reconstruction; see Fig. 9 for an example. In [72] an algorithm was provided that finds a minimal skeleton, if it exists. Subsequent encoding of the minimal skeleton transform using Elias codes resulted in higher compression than either optimum block-Huffman or optimum runlength-Huffman coding of the original image.

A generalization of the morphological skeleton transform uses different structuring elements A_n for each skeletonization step [64, p. 191]. In this case, nB in (33) and (34) is replaced with $A_0 \oplus A_1 \oplus \cdots \oplus A_n$. A general approach for morphological skeleton-like image representations with varying structuring elements was developed in [41]. Some recent research related to morphological skeletonization includes: shape decomposition based on iterative differences between image parts and maximal openings [97]; shape matching based on features extracted from the S_n [143]; symbolic image modeling [66]; vectorized skeleton coding [13]; and extension of binary skeleton coding ideas to coding gray-level images by first decomposing them into a collection of threshold binary images [103]. Finally, note that the morphological skeleton defined above is not necessarily connected; for *connected* skeletons see [3].

Gray-level Images: In [96] the skeleton transform has been extended to gray-level images. We describe this algorithm using terminology analogous to that for binary morphological skeletons. Namely, the nth skeleton component of f with respect to a binary structuring element B is the nonnegative function

$$s_n(f) = (f \ominus nB) - [(f \ominus nB) \circ B], \quad 0 \le n \le N, \tag{35}$$

where $N = \max\{n: f \ominus nB \neq 0\}$. A skeleton of f can be defined as the pointwise sum

$$SK(f) = \sum_{n=0}^{N} s_n(f). \tag{36}$$

As for binary images, f can be reconstructed from its components s_n either exactly or partially (its openings) [64], [69]. In [76] it was shown that the above skeleton obeys a threshold sum-superposition

$$SK(f) = \sum_{a} SK(f_a), \tag{37}$$

As in (30), this result reduces the analysis and implementation of gray-level skeletons to the much simpler binary skeletons $SK(f_a)$ of threshold binary images f_a.

For more general gray-level skeletons see [64], [66], [69] and for thinning gray-level images see [32], [39].

C. Shaped-Size Distributions

Matheron [80], [81] considered families of openings and closings of compact sets $X \subseteq \mathbf{R}^2$ by convex compact struc-

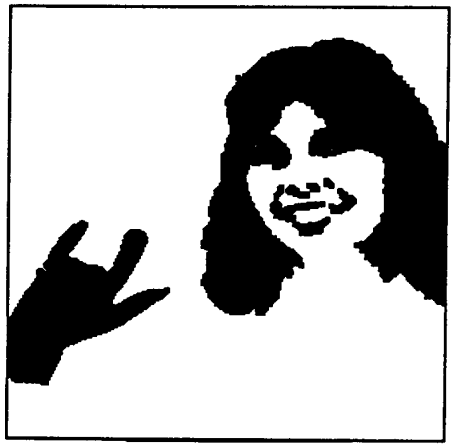

(a)

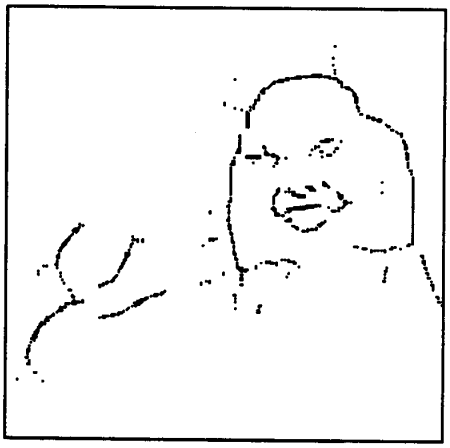

(b)

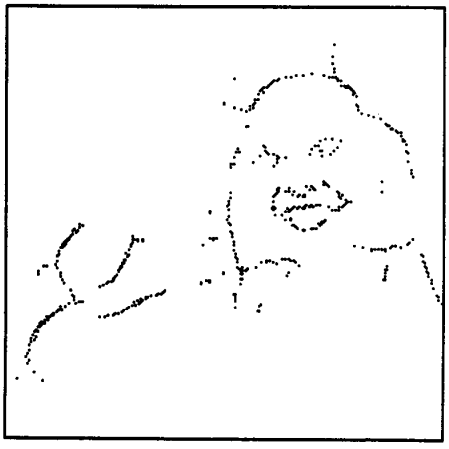

(c)

Fig. 9. (a) Original binary image (256 × 256 pixels). (b) Morphological skeleton with respect to a 3 × 3-pixel square structuring element. (c) Minimal skeleton. (From [72])

turing elements, e.g., disks rD of radius r, for unifying all sizing (sieving) operations in Euclidean spaces. He called these parametric openings *granulometries* and their areas *size distributions*. The decreasing function $A(X \circ rD)/A(X)$, $r \geq 0$, where $A(\cdot)$ denotes area, was related in [80], [81] to probabilistic measures of the size distribution in X. Serra and his co-workers [115, ch. 10] have used extensively these size distributions in image analysis applications to petrography and biology. In [64], [65], [69] Maragos related these size distributions to a concept of a pattern spectrum. Next we discuss these ideas only for discrete binary images.

The *pattern spectrum* of a discrete binary finite image $X \subseteq \mathbf{Z}^2$ relative to a structuring element $B \subseteq \mathbf{Z}^2$ is defined [69] as the differential size distribution function

$$PS_X(n, B) = A[X \circ nB \setminus X \circ (n+1)B]$$
$$= A(X \circ nB) - A[X \circ (n+1)B] \quad (38)$$

The rationale behind the symbolic term "pattern spectrum" is the fact that the opening $X \circ nB$ is the union of all $(nB + z)$ with $(nB + z) \subseteq X$, that is, of all shifted patterns B of size n that can fit inside X. Thus $A(X \circ nB)$ is a measure of the pattern content of X relative to the pattern nB, and (38) measures the change of such pattern content with respect to n. In actuality, the pattern spectrum, which is a nonnegative function for all B and n, is a *shape-size histogram*. It also has some conceptual similarities with the Fourier spectrum. The pattern spectrum conveys several types of information useful for shape description and multiscale image analysis. For example, the *boundary roughness* of X relative to B manifests itself as contributions in the lower-size part of the pattern spectrum. Long capes or bulky protruding parts in X that consist of patterns sB show up as isolated impulses in the pattern spectrum around positive $n = s$. Finally, the pattern spectrum can be defined for "negative" sizes by using closings instead of openings; in this case impulses at negative sizes indicate the existence of prominent intruding *gulfs* or *holes* in X.

Observe from (34) that $S_n = \varnothing$ implies that $X \circ nB = X \circ (n+1)B$; further, for $1 \leq k \leq N$,

$$X = X \circ kB \Leftrightarrow PS_X(n, B) = 0 \quad 0 \leq n < k. \quad (39)$$

Thus X is smooth to a degree k relative to B (i.e., $X = X \circ kB$) if and only if its first k pattern spectrum samples are zero, or if its first k skeleton components are empty.

In the theory [81], [115] of random stationary sets $X \subseteq \mathbf{Z}^2$, the size function $\lambda_x(z) = \max\{n: z \in X \circ nB\}$, $z \in X$, can be viewed as a random variable. Its probability function $p_k = \text{Prob}\{\lambda(z) = k\}$ is equal to $PS_x(k, B)/A(X)$. As explained in [69],

$$H(X/B) = -\sum_{n=0}^{N} p_n \log p_n \quad (40)$$

is the average uncertainty (entropy) of λ. It can be viewed as the *average roughness* of X relative to B, because it quantifies the shape-size complexity of X by measuring its boundary roughness averaged over all depths that B reaches. Thus $H(X/B)$ is maximum ($\log(N+1)$) iff X contains maximal patterns nB at equal area portions in all sizes n, and minimum (0) iff X is the union of maximal patterns of only one size.

All the above ideas can be extended to gray-level images [65], [69]. In [15] the normalized pattern spectrum (called "pecstrum") was used for binary and gray-level shape recognition by computing Euclidean distances between pattern spectra of test images and reference images. Some work related to morphological size distributions can also be found in [132], [135].

C. Fractals

1) Estimating Fractal Dimension: A large variety of natural image objects (e.g., clouds, coastlines, mountains, islands, trees, leaves, etc.) can be modeled very well with *fractals* [62]. Fractals are mathematical sets with very high level of geometrical complexity; formally, their Hausdorff dimension is larger than their topological dimension. An important characteristic of fractals to measure for purposes of shape description or classification is their fractal dimension. Among the various methods [62] to estimate the *fractal dimension* D of the fractal surface of a 3-dim set F, the *covering method* is based conceptually on Minkowski's idea of finding the area of irregular sets: dilate them with spheres of radius r, find the volume $V(r)$ of the dilated set, and set its area equal to $\lim_{r \to 0} A(r)$, where $A(r) = V(r)/2r$. If the surface of F is a pure fractal, then its area $A(r)$ at different scales r behaves as

$$\log A(r) = (2 - D) \log (r) + \text{constant}. \quad (41)$$

Thus, the fractal dimension D can be estimated by fitting a straight line to a log-log plot of $A(r)$. Digital implementations and variations of the above method can be found in [25], [26], [75], [95], [119] where morphological dilations and erosions are used to create a volume-blanket as a layer either covering or being peeled off from the intensity image surface at various scales.

Similarly, if F is a 2-dim set, e.g., the graph of a 1-dim signal, we can dilate it with disks of radius r, find the area $A(r)$ of the dilated set, and compute a multiscale length $L(r) = A(r)/2r$; then, for pure fractals.

$$\log L(r) = (1 - D) \log (r) + \text{constant}. \quad (42)$$

Figure 10(a) shows an intensity image profile (the solid line) and two layers of dilations (2 dotted lines) and erosions (2 dashed lines), both at scales $r = 10$ and 20. For "real world" signals with some fractal structure, the assumption of exact self-similarity at all scales is not true. Hence, to estimate a fractal dimension for the 1-dim signal of Fig. 10(a) we fit *locally* line segments on the log-log plot of $L(r)$. Figure 10b shows the local fractal dimension, which for each r is equal to one minus the slope of a line segment fitted (using linear regression) to the log-log plot of $L(r)$ over a moving window $[r, r + 9]$ of 10 scales. The relative variation of these local estimates indicate that, for real world signals relation (42) is only approximately true; hence, it is more meaningful to estimate their fractal dimension over a small finite range of scales.

2) Modeling Fractals: Currently, there are many computer algorithms to *generate* fractals. However, the *inverse problem*, i.e., given a fractal image find a signal model and an algorithm to generate it, is much more important and very difficult. Toward solving this inverse problem, Barnsley [5] and his co-workers developed the theory of *iterated function systems*. A key idea is their *collage theorem*, which states that if we can "closely" cover a binary fractal image F with a collage of m small patches that are reduced distorted copies of F, then we can reconstruct F (within arbi-

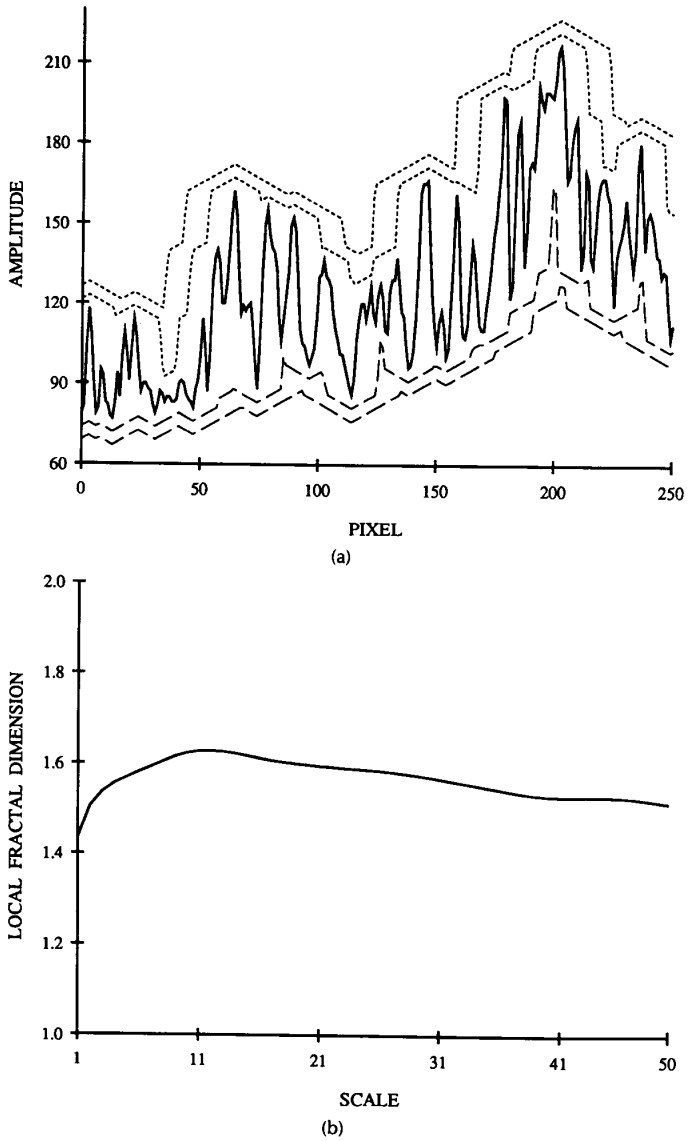

Fig. 10. (a) Discrete intensity image profile f (in solid line) with its erosions $f \ominus rg$ (dashed lines) and dilations $f \oplus rg$ (dotted lines) at scales $r = 10, 20$. The structuring function g was equal to $g(0) = 0.5$, $g(-1) = g(1) = 0$, and $g(n) = -\infty$ for $n \neq -1, 0, 1$. (b) Local fractal dimensions over a moving window of 10 scales.

trary accuracy) as the attractor of a set of m contractive affine maps (each map is responsible for one patch). Simple choices for these maps w_i, $1 \leq i \leq m$, are

$$w_i \begin{pmatrix} x \\ y \end{pmatrix} = r_i \cdot \begin{bmatrix} \cos\theta_i & -\sin\theta_i \\ \sin\theta_i & \cos\theta_i \end{bmatrix} \begin{bmatrix} x \\ y \end{bmatrix} + \begin{bmatrix} t_{xi} \\ t_{yi} \end{bmatrix}.$$

Each w_i, operating on all points (x, y) of F, gives a version of F that is rotated by angle θ_i, shrunk by a scale factor r_i, and translated by the vector (t_{xi}, t_{yi}). This theorem and a related synthesis algorithm have been very successful for fractal image modeling [5]. However, they require considerable human intervention. The difficulty lies in finding appropriate maps w_i, which (by variation of their scaling, rotation, and translation parameters) can collage F well. An approximate solution to this problem has been provided by Libeskind-Hadas and Maragos [59] who used the morphological skeleton transform to efficiently extract the parameters of these affine maps. In their work, a major skeleton branch was associated with each map w_i. The rotation angle θ_i was found as the angle that the skeleton branch forms with the horizontal. The translation vector (t_{xi}, t_{yi}) was taken as the vector of pixel coordinates of the skeleton branch point b. Finally, the scaling factor was set equal to $r = n/N$, where n is the index of the skeleton subset containing b. This algorithm can model images F that exhibit some degree of self-similarity; i.e., when local details of F closely resemble F as a whole.

V. Representation Theorems

Several mathematical structures, known as *image algebras*, have been developed in [21], [30], [50], [84], and [105]–[107]. Their purpose is to represent many image processing operators as a finite composition of a few basic operations including erosions and dilations. The image algebras in [30], [105], [107] encompass all linear (e.g., matrix operations) and many nonlinear image operators. Although erosions and dilations are insufficient by themselves to represent all possible image operations [107], it is abundantly clear from Sections III and IV that morphological operations can be combined in many ways to solve problems in a wide variety of applications. Hence, it is interesting to know which signal processing systems can be represented morphologically. Toward this goal, a theory was introduced in [64], [68], [70] that unifies many concepts encountered in signal processing or image analysis and represents a broad class of nonlinear and linear operators as a minimal combination of morphological erosions or dilations. Here we summarize the main results of this theory, in a simplified way, restricting our discussion only to signals with *discrete* domain $\mathbf{E} = \mathbf{Z}^d$. (The corresponding part of the theory for continuous-domain signals is contained in [64], [68]).

Consider an SP operator Ψ defined on the class $\mathcal{S}$ of all subsets of $\mathbf{E}$. Ψ is called *translation-invariant* iff $\Psi(X + p) = \Psi(X) + p$, for all $X \in \mathcal{S}$ and $p \in \mathbf{E}$. Any such Ψ is uniquely characterized by its *kernel* that is defined in [81] as the subclass $\mathcal{K}(\Psi) = \{X \in \mathcal{S} : 0 \in \Psi(X)\}$ of input sets. That is, the kernel is a collection of *input* sets such that their corresponding outputs contain the origin. Ψ is called *increasing* iff $A \subseteq B \Rightarrow \Psi(A) \subseteq \Psi(B)$. The *dual* SP operator of Ψ is defined as $\Psi^d(X) = [\Psi(X^c)]^c$, $X \in \mathcal{S}$, where $(\cdot)^c$ denotes set complementation. In [64], [68], [70], the kernel representation was extended to FP operators. A d-dim FP operator ψ is called *translation-invariant* iff $\psi[f(x - y) + c] = [\psi(f)](x - y) + c$, for all $(y, c) \in \mathbf{E} \times \mathbf{R}$ and $f(x) \in \mathcal{F}$, where $\mathcal{F}$ is the class of all functions with domain $\mathbf{E}$ and range $\mathbf{R} \cup \{\pm\infty\}$. That is, ψ is translation-invariant iff it commutes with a shift of both the argument and the amplitude of its input functions. Such a ψ is uniquely characterized by its *kernel*, which is defined as the subclass $\mathcal{K}(\psi) = \{f \in \mathcal{F} : [\psi(f)](0) \geq 0\}$ of input functions. Further, ψ is *increasing* iff $f \leq g \Rightarrow \psi(f) \leq \psi(g)$. The dual operator of ψ is defined as $\psi^d(f) = -\psi(-f)$, where $(-f)(x) = -f(x)$. The class of translation-invariant increasing SP or FP operators are useful because of the following two representation theorems.

THEOREM 1 (Matheron [81]). *Any translation-invariant increasing SP operator $\Psi: \mathcal{S} \to \mathcal{S}$ can be represented exactly as the union of erosions by its kernel sets and as the intersection of dilations by the reflected kernel sets of its dual operator Ψ^d.*

THEOREM 2 (Maragos [64], [68]). *Any translation-invariant increasing FP operator $\psi: \mathcal{F} \to \mathcal{F}$ can be represented exactly as the pointwise supremum of erosions by its kernel functions, and as the pointwise infimum of dilations by the reflected kernel functions of its dual operator ψ^d.*

The two theorems above require an infinite number of erosions to represent a given system. However, we can find more efficient (requiring fewer erosions) theorems by using only a substructure of the kernel. The pair $(\mathcal{K}(\Psi), \subseteq)$ is a partially ordered set with respect to set inclusion. A *minimal element* of $(\mathcal{K}(\Psi), \subseteq)$ is any set in $\mathcal{K}(\Psi)$ that is not preceded (with respect to $\subseteq$) by any other kernel set. The *basis* $\mathcal{B}(\Psi)$ of the translation-invariant operator Ψ is defined as the set of all its minimal kernel elements. It was shown in [64], [68] that $\mathcal{B}(\Psi)$ *exists* (i.e., is nonempty) if Ψ is increasing and upper semicontinuous. [An increasing SP operator Ψ is upper semicontinuous iff, for any decreasing set sequence (X_n) with $X_{n+1} \subseteq X_n$, $\Psi(\cap_n X_n) = \cap_n \Psi(X_n)$.] Similarly, the pair $(\mathcal{K}(\psi), \leq)$ is a partially ordered set with respect to the function ordering $\leq$. A minimal function-element of $(\mathcal{K}(\psi), \leq)$ is any function in $\mathcal{K}(\psi)$ that is not preceded (with respect to function $\leq$) by any other kernel function. Then, the *basis* $\mathcal{B}(\psi)$ of ψ is defined as the set of its minimal kernel functions, and it *exists* if ψ is increasing and upper semicontinuous [64], [68]. [An increasing FP operator ψ is upper semicontinuous iff, for any decreasing function sequence (f_n) with $f_{n+1} \leq f_n$, $\psi(\wedge_n f_n) = \wedge_n \psi(f_n)$.] The importance of the basis for SP of FP operators is revealed by the following two representation theorems.

THEOREM 3 (Maragos [64], [68]). *Any translation-invariant, increasing and upper semicontinuous SP operator $\Psi: \mathcal{S} \to \mathcal{S}$ can be represented exactly as the union of erosions by its basis sets. If the dual Ψ^d is upper semicontinuous, then Ψ can also be represented as the intersection of dilations by the reflected basis sets of Ψ^d.*

THEOREM 4 (Maragos [64], [68]). *(a)-(FP systems): Any translation-invariant, increasing and upper semicontinuous FP operator $\psi: \mathcal{F} \to \mathcal{F}$ can be represented exactly as the pointwise supremum of erosions by its basis functions. If the dual ψ^d is upper semicontinuous, then ψ can also be represented as the pointwise infimum of dilations by the reflected basis functions of ψ^d.*

(b)-(FSP systems). Let $\phi: \mathcal{F} \to \mathcal{F}$ be an FSP translation-invariant operator that commutes with thresholding, and let Φ be its respective SP operator. Then ϕ is exactly represented as the supremum of erosions by the basis sets of Φ. If the dual SP operator Φ^d is upper semicontinuous, then ϕ can also be represented as the infimum of dilations by the reflected basis sets of Φ^d.

In [73], [74] these very general theorems have been applied to various filters such as linear shift-invariant, morphological, median, rank-order, linear combinations of rank-order, and stack filters. Below we give some simple examples.

Example 1 (Linear Filters). A linear filter is translation-invariant and increasing iff its impulse response is everywhere nonnegative and has area equal to one. Consider the 2-point FIR filter $[\psi(f)](n) = af(n) + (1 - a) f(n - 1)$, where $0 < a < 1$. Then the basis of ψ consists of all functions $g(n)$ with $g(0) = r \in \mathbf{R}$, $g(-1) = -ar/(1 - a)$, and $g(n) = -\infty$ for $n \neq 0, -1$. Then Theorem 4(a) yields

$$af(n) + (1 - a) f(n - 1) = \sup_{r \in \mathbf{R}} \left[\min \left\{ f(n) - r, f(n - 1) + \frac{ar}{1 - a} \right\} \right], \quad (43)$$

which expresses a linear convolution as a supremum of erosions. FIR linear filters have an infinite basis, which forms a finite-dimensional vector space.

Example 2 (Median filters). Many discrete FSP increasing morphological filters and all rank-order filters have a finite number of minimal elements; hence, they can be expressed

as a finite max-of-erosions or min-of-dilations. Further, they commute with thresholding, which allows us to focus only on the SP versions of such filters. For example, the FSP median by the window $W = \{-1, 0, 1\}$ has an SP version of $\Phi(X) = \{ p \in \mathbf{Z}: |(X \cap W + p| \geq 2\}, X \subseteq \mathbf{Z}$. Φ has 3 basis sets: $\{-1, 0\}$, $\{-1, 1\}$, and $\{0, 1\}$. Hence, Theorem 4(b) yields

$$\text{med}\,[f(x-1), f(x), f(x+1)] = \max \begin{Bmatrix} \min\,[f(x-1), f(x)], \\ \min\,[f(x-1), f(x+1)], \\ \min\,[f(x), f(x+1)] \end{Bmatrix}. \quad (44)$$

Example 3 (Stack Filters). The definition of stack filters in (20) requires a *positive Boolean function* $\beta(x_1, \cdots, x_n)$. Such a function has an irreducible sum-of-products expression as Boolean sum of its prime implicants and an irreducible product-of-sums expression as Boolean product of its prime implicates [88]. In [134] all the 20 different stack filters with a β of $n = 3$ variables were examined in detail. For $n > 3$ there was not a direct way to find a functional definition of arbitrary stack filters. However, by using morphological concepts in [74] a general functional definition was obtained as follows. The positive Boolean function β corresponds uniquely to a translation-invariant increasing and upper semicontinuous SP operator Φ, which in turn defines uniquely an FSP operator ϕ that commutes with thresholding. That is, stack filters are the class of all discrete translation-invariant FSP finite-window filters that commute with thresholding. Given β, Φ is found by replacing Boolean AND/OR with set $\cap/\cup$; then, ϕ is obtained by replacing set $\cap/\cup$ in Φ with min/max. Further, as shown in [74], stack filters have a finite number of basis sets that are in one-to-one correspondence with the prime implicants of β. Thus the basis can be used to find the irreducible forms of β, and vice-versa. For example, the FSP opening $\phi(f) = f \circ A, A = \{-1, 0, 1\}$, can be viewed as a stack filter, whose functional definition is associated with the window $W = \{-2, -1, 0, 1, 2\}$. Its dual filter is the FSP closing $f \bullet A$. Let $\Phi(X) = X \circ A$ and $\Phi^d(X) = X \bullet A$ be its respective SP operator and dual SP operator. The basis sets of Φ are [64], [68] the 3 subsets $G_1 = A - 1$, $G_2 = A$, $G_3 = A + 1$ of W; the basis sets of Φ^d are the 4 subsets $H_1 = \{0\}$, $H_2 = \{-2, 1\}$, $H_3 = \{-1, 2\}$, $H_4 = \{-1, 1\}$ of W. Thus, from Theorem 4(b), ϕ can be realized as

$$f \circ A(x) = \max_{i=1}^{3} \left\{ \min_{y \in G_i} f(x+y) \right\} = \min_{k=1}^{4} \left\{ \max_{y \in H_k} f(x+y) \right\}. \quad (45)$$

The β corresponding to Φ and ϕ is $\beta(x_1, \cdots, x_5) = x_1x_2x_3 + x_2x_3x_4 + x_3x_4x_5 = x_3(x_1 + x_4)(x_2 + x_4)(x_2 + x_5)$. Thus there is one-to-one correspondence between the 3 prime implicants of β and the erosions (local min) by the basis sets of Φ, as well as between the 4 prime implicates of β and the dilations (local max) by the basis sets of Φ^d. Thus stack filters can be expressed as minimal forms of max-min operations based either on irreducible forms of their Boolean function or on their minimal kernel elements. In [74] both approaches were compared, and their theoretical equivalence was established.

Example 4 (Hybrid Linear/Nonlinear filters). There are many nonlinear filters that have both a linear and nonlinear (i.e., rank-order) component, e.g., [4], [6], [12], [22], [48], [94], [127]. They are useful because they combine desirable characteristics of both linear and nonlinear filters. The representation theory in this section applies to these filters too, if their linear parts contain positive coefficients which sum to one. A simple such filter is the *Wilcoxon* filter [22]

$$[\psi(f)](n) = \text{median}\,\{[f(n-2) + f(n+2)]/2, [f(n-1) + f(n+1)]/2, f(n)\}, \quad (46)$$

whose basis is obtained by combining results (43) and (44); see also [64, p. 157].

The above examples show the power of the general representation theorems. An interesting area of current research is concerned with using these results as a basis for a design methodology for morphological systems.

Conclusions

In this paper we have attempted to show how a wide range of multidimensional signal processing problems can be addressed using morphological systems. We have shown that simple nonlinear operators such as erosion and dilation can be combined to create many different types of signal processing and analysis operators. A major advantage of morphological systems is their built-in ability to represent and extract shape in multidimensional signals. Another advantage is that they are well suited for simple and efficient implementations using parallel or sequential computation.

So far, many of the signal processing algorithms and analysis techniques based on morphological systems have been derived heuristically or experimentally. However, the existence of powerful representation theorems for morphological systems suggests that much more can be done to develop methodologies for designing systems of this class. The results of research in this area will impact many areas of application of multidimensional signal processing.

Appendix

Historical Notes on Definitions and Notation

Considerable confusion has arisen regarding the definitions of the basic operations of mathematical morphology. This confusion is primarily due to usage of the symbols $\oplus$ and $\ominus$ by different authors to mean different things. In [42] Hadwiger's definition of Minkowski set addition [85] was identical to our definition (4) of set dilation. Our definition of set erosion (5) is identical to an operation introduced by Hadwiger [42] and called Minkowski set subtraction. Thus, in this paper, set dilation and erosion are identical to the classical Minkowski set addition and Minkowski set subtraction. These definitions were used by Sternberg [120]–[122] in his contributions to the field.

Matheron [81] and Serra [115] used the *reflection* $\check{B} = \{-b: b \in B\}$ of B to define the set of basic operations of mathematical morphology in a somewhat different way. Minkowski addition was defined identically to Hadwiger's definition, and the symbol $\oplus$ was used for this operation. Minkowski subtraction was redefined as $X \ominus B = \cap_{b \in B}(X + b) = \{z: (\check{B} + z) \subseteq X\}$, which is the same as Hadwiger's definition except the structuring set is reflected. Matheron and Serra defined the dilation of X by B as $X \oplus \check{B} = \{z: (B + z) \cap X \neq 0\}$ where $\oplus$ means Minkowski set addition.

They defined erosion of X by B as $X \ominus \check{B} = \{z:(B + z) \subseteq X\}$, where $\ominus$ means their redefined Minkowski set subtraction (i.e., with the reflected set), thereby creating part of the confusion. Thus the two reflections cancel and the Matheron/Serra definition of erosion turns out to be identical to the classical Minkowski set subtraction, and thus, identical to the definition of this paper. Serra introduced also the *hit-or-miss* transform, which is a generalization of erosion as a Boolean matched filter. The Matheron/Serra definitions of opening and closing of X by B are $X_B = (X \ominus \check{B}) \oplus B$ and $X^B = (X \oplus \check{B}) \ominus B$. Their opening involves the same operations and gives identical result to the definition that we have presented; i.e., $X_B = X \circ B$. However, their closing by B is equivalent to our closing by the reflected B; i.e., $X^B = X \bullet \check{B}$.

In [70]–[74] we used Matheron and Serra's definitions. However, in this paper we have adopted Sternberg's definitions and his terminology (i.e., defining dilation and erosion identically to Minkowski addition and subtraction), because they are somewhat simpler. (The Matheron and Serra definitions have certain advantages in terms of duality properties). Note that Matheron and Serra's definitions become identical to Sternberg's if $B = \check{B}$, i.e., if the structuring element is symmetric. In addition we use the notation $\circ$ and $\bullet$ for opening and closing as in [43], and the group-theoretic notation $X + b$ for set translation as in [28].

References

[1] R. S. Acharya and R. Laurette, "Mathematical morphology for 3-D image analysis," in *Proc. ICASSP-88*, New York, April 1988.

[2] G. R. Arce, N. C. Gallagher, and T. A. Nodes, "Median filters: Theory for one- and two-dimensional filters," in *Advances in Computer Vision and Image Processing*, Vol. 2, T. S. Huang, Ed. CT: JAI Press, 1986.

[3] C. Arcelli, L. Cordella, and S. Levialdi, "From local maxima to connected skeletons," *IEEE Trans. Pattern Anal. Mach. Intellig.*, PAMI-3, pp. 134–143, Mar. 1981.

[4] J. Astola and O. Yli-Harja, "Gradient median filter," in *Proc. IEEE ISCAS-87*, Philadelphia, PA, May 1987.

[5] M. Barnsley, *Fractals Everywhere*. NY: Acad. Press, 1988.

[6] J. B. Bednar and T. L. Watt, "Alpha-trimmed means and their relationship to median filters," *IEEE Trans. Acoust. Speech, Signal Process.*, ASSP-32, pp. 145–153, Feb. 1984.

[7] H. Blum, "A Transformation for extracting new descriptions of shape," in *Models for the Perception of Speech and Visual Forms*, W. Wathen-Dunn, Ed. Cambridge, MA: MIT Press, 1967.

[8] ——, "Biological shape and visual senses (Part I)," *J. Theor. Biol.*, vol. 38, pp. 205–287, 1973.

[9] G. Borgefors, "Distance transformations in arbitrary dimensions," *Comp. Vision Graph. Image Process.*, 27, pp. 321–345, 1984.

[10] N. K. Bose, *Applied Multidimensional Systems Theory*. NY: Reinhold, 1982.

[11] ——, *Digital Filters: Theory and Applications*. Elsevier, 1985.

[12] A. C. Bovik, T. S. Huang, and D. C. Munson, Jr., "A generalization of median filtering using linear combinations of order statistics," *IEEE Trans. Acoust. Speech, Signal Process.*, ASSP-31, pp. 1342–1349, Dec. 1983.

[13] J. W. Brandt and A. K. Jain, "A medial axis transform algorithm for compression and vectorization of document images," in *Proc. IEEE ICASSP-89*, Glasgow, Scotland, May 1989.

[14] R. W. Brockett, Lectures in Nonlinear Science, UC Berkeley Summer School, 1987.

[15] J. F. Bronskill and A. N. Venetsanopoulos, "Multidimensional shape description and recognition using mathematical morphology," *J. Intellig. Rob. Syst.*, 1, pp. 117–143, 1988.

[16] P. J. Burt and E. H. Adelson, "The Laplacian pyramid as a compact image code," *IEEE Trans. Commun.*, COM-31, pp. 532–540, Apr. 1983.

[17] A. R. Butz, "A class of rank order smoothers," *IEEE Trans. Acoust. Speech, Signal Process.*, ASSP-34, pp. 157–165, Feb. 1986.

[18] M. Chen and P. Yan, "A multiscaling approach based on morphological filtering," *IEEE Trans. Pattern Anal. Mach. Intell.*, PAMI-11, pp. 694–700, July 1989.

[19] C. H. Chu and E. J. Delp, "Impulsive noise suppression and background normalization of electrocardiogram signals using morphological operators," *IEEE Trans. Biomed. Enginr.*, BME-36, pp. 262–273, Feb. 1989.

[20] E. J. Coyle, "Rank order operators and the mean absolute error criterion," *IEEE Trans. Acoust. Speech Signal Process.*, vol. ASSP-36, pp. 63–76, Jan. 1988.

[21] T. R. Crimmins and W. R. Brown, "Image algebra and automatic shape recognition," *IEEE Trans. Aerosp. and Electron. Syst.*, vol. AES-21, pp. 60–69, Jan. 1985.

[22] R. J. Crinon, "The Wilcoxon filter: A robust filtering scheme," in *Proc. IEEE ICASSP-85*, Tampa, FL, Mar. 1985.

[23] P.-E. Danielsson and S. Levialdi, "Computer architectures for pictorial information systems," *IEEE Computer Mag.*, Nov. 1981, pp. 53–67.

[24] A. M. Darwish and A. K. Jain, "A rule based approach for visual pattern inspection," *IEEE Trans. Pattern Anal. Mach. Intellig.*, PAMI-10, pp. 56–68, Jan. 1988.

[25] B. Dubuc, C. Roques-Carmes, C. Tricot, and S. W. Zucker, "The variation method: a technique to estimate the fractal dimension of surfaces," in *Proc. SPIE 845: Visual Communications and Image Processing II*, 1987.

[26] B. Dubuc, J. F. Quiniou, C. Roques-Carmes, C. Tricot, and S. W. Zucker, "Evaluating the fractal dimension of profiles," *Phys. Rev. A*, vol. 39, pp. 1500–1512, Feb. 1989.

[27] D. E. Dudgeon and R. M. Mersereau, *Multidimensional Digital Signal Processing*. Englewood Cliffs, NJ: Prentice-Hall, 1984.

[28] E. R. Dougherty and C. R. Giardina, *Image Processing-Continuous to Discrete*. Englewood Cliffs, NJ: Prentice-Hall, 1987.

[29] ——, "Error bounds for morphologically derived measurements," *SIAM J. Appl. Math.*, 47, pp. 425–440, Apr. 1987.

[30] ——, "Image Algebra-induced operators and induced subalgebras," in *Proc. SPIE 845: Visual Communications and Image Processing II*, 1987.

[31] M. J. B. Duff, D. M. Watson, T. J. Fountain, and G. K. Shaw, "A cellular logic array for image processing," *Pattern Recogn.*, vol. 5, pp. 229–247, 1973.

[32] C. R. Dyer and A. Rosenfeld, "Thinning algorithms for gray-scale pictures," *IEEE Trans. Pattern Anal. Mach. Intellig.*, PAMI-1, pp. 88–89, Jan. 1979.

[33] T. Esselman and J. G. Verly, "Applications of mathematical morphology to range imagery," MIT Lincoln Lab Tech. Rep. 797, Dec. 1987.

[34] A. G. Fabbri, *Image Processing of Geological Data*. NY: Reinhold, 1984.

[35] R. J. Feehs and G. R. Arce, "Multidimensional morphological edge detection," in *Proc. SPIE 845: Visual Communications and Image Processing II*, 1987.

[36] J. P. Fitch, E. J. Coyle, and N. C. Gallagher, Jr., "Median filtering by threshold decomposition," *IEEE Trans. Acoust., Speech, Signal Processing*, ASSP-32, pp. 1183–1188, Dec. 1984.

[37] ——, "The analog median filter," *IEEE Trans. Circ. Syst.*, CAS-33, pp. 94–102, Jan. 1986.

[38] N. C. Gallagher, Jr. and G. L. Wise, "A theoretical analysis of the properties of median filters," *IEEE Trans. Acoust. Speech, Signal Process.*, ASSP-29, pp. 1136–1141, Dec. 1981.

[39] V. Goetcherian, "From binary to grey tone image processing using fuzzy logic concepts," *Pattern Recognition*, vol. 12, pp. 7–15, 1980.

[40] M. J. E. Golay, "Hexagonal parallel pattern transformations," *IEEE Trans. Comput.*, C-18, pp. 733–740, Aug. 1969.

[41] J. Goutsias and D. Schonfeld, "Image coding via morphological transformations: A general theory," in *Proc. IEEE Conf. CVPR-89*, San Diego, CA, June 1989.

[42] H. Hadwiger, *Vorlesungen über Inhalt, Oberfläche, und Isoperimetrie*. Berlin: Springer Verlag, 1957.

[43] R. M. Haralick, S. R. Sternberg, and X. Zhuang, "Image analysis using mathematical morphology," *IEEE Trans. Pattern Anal. Mach. Intell.*, PAMI-9, pp. 532–550, July 1987.
[44] R. M. Haralick, C. Lin, J. S. J. Lee, and X. Zhuang, "Multiresolution morphology," in *Proc. 1st ICCV*, London, 1987.
[45] R. M. Haralick, X. Zhuang, C. Lin, and J. S. J. Lee, "The digital morphological sampling theorem," *IEEE Trans. Acoust., Speech, Signal Process.*, vol. ASSP-37, pp. 2067–2090, Dec. 1989.
[46] R. G. Harber, S. C. Bass, and G. W. Neudeck, "VLSI implementation of a fast rank order filtering algorithm," in *Proc. IEEE ICASSP-85*, Tampa, FL, Mar. 1985.
[47] H. J. A. M. Heijmans and C. Ronse, "The algebraic basis of mathematical morphology Part I: Dilations and erosions," Rep. AM-R8807, CWI, Amsterdam, June 1988.
[48] P. Heinonen and Y. Neuvo, "FIR-median hybrid filters," *IEEE Trans. Acoust. Speech, Signal Processing*, ASSP-35, pp. 832–838, June 1987.
[49] J. M. Hereford and W. T. Rhodes, "Nonlinear Optical Image Filtering by Time-Sequential Threshold Decomposition," *Optical Enginr.*, Apr. 1988.
[50] K. S. Huang, B. K. Jenkins, and A. A. Sawchuk, "Binary image algebra and optical cellular logic processor design," *Comp. Vision Graph. Image Process.*, 45, pp. 295–345, 1989.
[51] B. I. Justusson, "Median filtering: statistical properties," in *Two-Dimensional Digital Signal Processing II: Transforms and Median Filters*, T. S. Huang, Ed. NY: Springer Verlag, 1981.
[52] A. Kaufmann, *Introduction to the Theory of Fuzzy Subsets*. NY: Acad. Press, 1975.
[53] R. A. Kirsch, L. Cahn, C. Ray, and G. H. Urban, "Experiments in processing pictorial information with a digital computer," in *Proc. Eastern Joint Comput. Conf.*, 1957.
[54] J. C. Klein and J. Serra, "The texture analyzer," *J. Microscopy*, vol. 95, pt. 2, pp. 349–356, Apr. 1972.
[55] C. Lantuejoul, "Skeletonization in quantitative metallography," in *Issues of Digital Image Processing*, R. M. Haralick and J. C. Simon, Eds. Groningen, The Netherlands: Sijthoff and Noordhoff, 1980.
[56] C. Lantuejoul and J. Serra, "M-Filters," in *Proc. IEEE ICASSP-82*, Paris, May 1982.
[57] J. S. J. Lee, R. M. Haralick, and L. G. Shapiro, "Morphologic edge detection," *IEEE Trans. Rob. Autom.*, vol. RA-3, pp. 142–156, Apr. 1987.
[58] Y. H. Lee and S. A. Kassam, "Generalized median filtering and related nonlinear filtering techniques," *IEEE Trans. Acoust. Speech, Signal Process.*, ASSP-33, pp. 672–683, June 1985.
[59] R. Libeskind-Hadas and P. Maragos, "Application of iterated function systems and skeletonization to synthesis of fractal images," in *Proc. SPIE 845: Visual Communications and Image Processing II*, 1987.
[60] H. G. Longbotham and A. C. Bovik, "Relating analog and digital order statistic filters," in *Proc. IEEE ICASSP-88*, New York, Apr. 1988.
[61] R. M. Lougheed, D. L. McCubbrey, and S. R. Sternberg, "Cytocomputers: Architectures for parallel image processing," in *Proc. Workshop Picture Data Descr. Manag.*, Pacific Grove, CA, 1980.
[62] B. B. Mandelbrot, *The Fractal Geometry of Nature*. San Francisco, Freeman, 1982.
[63] J. R. Mandeville, "Novel Method for Analysis of Printed Circuit Images," *IBM J. Res. Develop.*, vol. 29, pp. 73–86, Jan. 1985.
[64] P. Maragos, "A unified theory of translation-invariant systems with applications to morphological analysis and coding of images," Ph.D. dissertation, School Electr. Enginr., Georgia Inst. Technology, Atlanta, GA, July 1985.
[65] ——, "Morphology-based multidimensional signal processing," in *Proc. 21st Annual Conf. Inform. Sci. Syst.*, Johns Hopkins Univ., Baltimore, MD, Mar. 1987.
[66] ——, "Morphology-based symbolic image modeling, multiscale nonlinear smoothing, and pattern spectrum," in *Proc. IEEE Conf. CVPR-88*, Ann Arbor, MI, June 1988.
[67] ——, "Morphological correlation and mean absolute error criteria," in *Proc. IEEE ICASSP-89*, Glasgow, Scotland, May 1989.
[68] ——, "A representation theory for morphological image and signal processing," *IEEE Trans. Pattern Anal. Mach. Intellig.*, PAMI-11, pp. 586–599, June 1989.
[69] ——, "Pattern spectrum and multiscale shape representation," *IEEE Trans. Pattern Anal. Mach. Intellig.*, PAMI-11, pp. 701–716, July 1989.
[70] P. Maragos and R. W. Schafer, "A Unification of Linear, Median, Order-Statistics, and Morphological Filters under Mathematical Morphology," in *Proc. IEEE ICASSP-85*, Tampa, FL, March 1985.
[71] ——, "Applications of morphological filtering to image processing and analysis," in *Proc. IEEE ICASSP-86*, Tokyo, April 1986.
[72] ——, "Morphological skeleton representation and coding of binary images," *IEEE Trans. Acoust., Speech, Signal Process.*, ASSP-34, Oct. 1986, pp. 1228–1244.
[73] ——, "Morphological filters—Part I: Their set-theoretic analysis and relations to linear shift-invariant filters," *IEEE Trans. Acoust. Speech, Signal Processing*, ASSP-35, pp. 1153–1169, Aug. 1987.
[74] ——, "Morphological filters—Part II: Their relations to median, order-statistic, and stack filters," *IEEE Trans. Acoust. Speech, Signal Process.*, ASSP-35, pp. 1170–1184, Aug. 1987. Also "Corrections," *ibid*, ASSP-37, p. 597, Apr. 1989.
[75] P. Maragos and F. K. Sun, "Measuring fractal dimension: Morphological estimates and iterative optimization," in *Proc. SPIE 1199: Visual Communications and Image Processing*, Nov. 1989.
[76] P. Maragos and R. D. Ziff, "Threshold parallelism im morphological feature extraction, skeletonization, and pattern spectrum," in *Proc. SPIE 1001: Visual Communications and Image Processing*, 1988.
[77] M. Maresca and H. Li, "Morphological operations on mesh connected architecture: A generalized convolution algorithm," in *Proc. IEEE Conf. CVPR-86*, Miami, FL, June 1986.
[78] D. Marr, *Vision*. San Francisco, Freeman, 1982.
[79] D. Marr and E. Hildreth, "Theory of edge detection," *Proc. R. Soc. Lond. B 207*, pp. 187–217, 1980.
[80] G. Matheron, *Élements pour une Théorie des Milieux Poreux*. Paris: Masson, 1967.
[81] ——, *Random Sets and Integral Geometry*. NY: J. Wiley, 1975.
[82] F. Meyer, "Contrast feature extraction," in *Special Issues of Practical Metallography*. Stuttgart: Riederer Verlag GmbH, 1978. (Proc. 2nd European Symp. on Quant. Anal. of Microstruct. in Materials Science, Biology and Medicine, France, Oct. 1977.)
[83] ——, "Iterative image transformations for an automatic screening of cervical smears," *J. Histochem. and Cytochem.*, vol. 27, 1979, pp. 128–135.
[84] P. E. Miller, "Development of a mathemtical structure for image processing," Perkin-Elmer Optic. Div. Tech. Rep., 1983.
[85] H. Minkowski, "Volumen und Oberflache," *Math. Annalen*, vol. 57, pp. 447–495, 1903.
[86] G. A. Moore, "Automatic scanning and computer processes for the quantitative analysis of micrographs and equivalent subjects," in *Pictorial Pattern Recognition*, G. C. Cheng *et al.*, Eds. Washington, DC: Thompson, 1968.
[87] J. C. Mott-Smith, "Medial axis transformations," in *Picture Processing and Psychopictorics*, B. S. Lipkin and A. Rosenfeld, Eds. NY: Acad. Press, 1970.
[88] S. Muroga, *Threshold Logic and Its Applications*. NY: Wiley, 1971.
[89] Y. Nakagawa and A. Rosenfeld, "A note on the use of local min and max operations in digital picture processing," *IEEE Trans. Syst., Man, and Cybern.*, SMC-8, 1978.
[90] J. A. Noble, "Morphological feature detectors," in *Proc. 2nd ICCV*, Trapon Springs, FL, Dec. 1988.
[91] T. A. Nodes and N. C. Gallagher, Jr., "Median filters: Some modifications and their properties," *IEEE Trans. Acoust. Speech Signal Process.*, ASSP-30, pp. 739–746, Oct. 1982.
[92] E. Ochoa, J. P. Allebach, and D. W. Sweeney, "Optical median filtering by threshold decomposition," *Appl. Opt.*, 26, pp. 252–260, Jan. 1987.
[93] A. V. Oppenheim and R. W. Schafer, *Discrete-time Signal Processing*. Englewood Cliffs, NJ: Prentice-Hall, 1989.
[94] F. Palmieri and C. G. Boncelet, Jr., "*Ll* filters—a new class of

order statistic filters," *IEEE Trans. Acoust. Speech Signal Process.*, ASSP-37, pp. 691–701, May 1989.
[95] S. Peleg, J. Naor, R. Hartley, and D. Avnir, "Multiple resolution texture analysis and classification," *IEEE Trans. Pattern. Anal. Mach. Intell.*, PAMI-6, pp. 518–523, July 1984.
[96] S. Peleg and A. Rosenfeld, "A min-max medial axis transformation," *IEEE Trans. Pattern. Anal. Mach. Intell.*, vol. PAMI-3, pp. 208–210, Mar. 1981.
[97] I. Pitas and A. N. Venetsanopoulos, "Shape decomposition by mathematical morphology," in *Proc. 1st ICCV*, London, 1987.
[98] W. K. Pratt, *Digital Image Processing*. NY: Wiley, 1978.
[99] K. Preston, Jr., "Feature extraction by Golay hexagonal pattern transforms," *IEEE Trans. Comput.*, C-20, pp. 1007–1014, Sep. 1971.
[100] ——, "Σ-Filters," *IEEE Trans. Acoust., Speech, and Signal Process.*, ASSP-31, pp. 861–876, Aug. 1983.
[101] K. Preston, Jr., M. J. B. Duff, S. Levialdi, P. E. Norgren, and J.-I. Toriwaki, "Basics of cellular logic with some applications in medical image processing," *Proc. IEEE*, vol. 67, pp. 826–856, May 1979.
[102] *Proc. IEEE Workshop CAPAIDM*, Miami FL, Nov. 1985.
[103] S. A. Rajala, H. A. Peterson, and E. J. Delp, "Binary morphological coding of grayscale images," in *Proc. IEEE ISCAS-88*, Espoo, Finland, June 1988.
[104] C. H. Richardson and R. W. Schafer, "Application of mathematical morphology to FLIR images," in *Proc. SPIE 845: Visual Communications and Image Processing II*, 1987.
[105] G. X. Ritter, and P. D. Gader, "Image algebra techniques for parallel image processing," *J. Paral. Distr. Comput.*, 4, 7–44, 1987.
[106] G. X. Ritter and J. N. Wilson, "Image algebra in a nutshell," in *Proc. 1st ICCV*, London, June 1987, pp. 641–645.
[107] G. X. Ritter, J. L. Davidson, and J. N. Wilson, "Beyond mathematical morphology," in *Proc. SPIE 845: Visual Communications and Image Processing II*, 1987.
[108] K. Rodenacker, P. Gais, U. Jutting, and G. Burger, "Mathematical morphology in grey images," in *Proc. 1983 European Signal Processing Conference*.
[109] J. B. T. M. Roerdink and H. J. A. M. Heijmans, "Mathematical morphology for structures without translation symmetry," *Signal Processing*, vol. 15, pp. 271–277, 1988.
[110] C. Ronse and H. J. A. M. Heijmans, "The algebraic basis of mathematical morphology. Part II: Openings and Closings," Manuscript M291, Philips Res. Lab, Brussels, Feb. 1989.
[111] A. Rosenfeld, Ed., *Multiresolution Image Processing and Analysis*. NY: Springer-Verlag, 1984.
[112] A. Rosenfeld and A. C. Kak, *Digital Picture Processing*. vols. 1 & 2. NY: Acad. Press, 1982.
[113] A. Rosenfeld and J. L. Pfaltz, "Sequential operations in digital picture processing," *J. ACM*, 13, pp. 471–494, Oct. 1966.
[114] J. Serra, "Morphologie Pour Les Fonctions: a peu pres en tout ou rien," Tech. Rep. 406-61, Centre de Morphologie Mathematique, Fontainebleau, 1975.
[115] ——, *Image Analysis and Mathematical Morphology*. NY: Acad. Press, 1982.
[116] ——, Ed., *Image Analysis and Mathematical Morphology*, Vol. 2: Theoretical Advances. NY: Acad. Press, 1988.
[117] F. Y.-C. Shih and O. R. Mitchell, "Threshold decomposition of gray-scale morphology into binary morphology," *IEEE Trans. Pattern Anal. Mach. Intellig.*, PAMI-11, pp. 31–42, Jan. 1989.
[118] M. M. Skolnick, "Application of morphological transformations to the analysis of two-dimensional electrophoretic gels of biological materials," *Comput. Vision, Graph., Image Process.*, **35**, pp. 306–332, 1986.
[119] M. C. Stein, "Fractal image models and object detection," in *Proc. SPIE 845: Visual Communications and Image Processing II*, 1987.
[120] S. R. Sternberg, "Parallel architectures for image processing," in *Proc. IEEE Conf. Comput. Softw. Applic.*, Chicago, 1979.
[121] ——, "Cellular computers and biomedical image processing," in *Biomedical Images and Computers*, J. Sklansky and J. C. Bisconte, Eds. Berlin: Springer Verlag, 1982. (Presented at US-France Seminar on Biomedical Image Processing, St. Pierre de Chartreuse, France, 1980.)
[122] ——, "Grayscale morphology," *Comput. Vision, Graph., Image Proc.* **35**, pp. 333–355, 1986.
[123] S. R. Sternberg and E. S. Sternberg, "Industrial inspection by morphological virtual gauging," in *Proc. IEEE Workshop Comput. Archit. Pattern Anal. Image Datab. Manag.*, Pasadena, CA, Oct. 1983.
[124] R. L. Stevenson and G. R. Arce, "Morphological filters: Statistics and further syntactic properties," *IEEE Trans. Circ. and Syst.*, CAS-34, pp. 1292–1305, Nov. 1987.
[125] F.-K. Sun and S. L. Rubin, "Algorithm development for autonomous image analysis based on mathematical morphology," in *Proc. SPIE 845: Visual Communications and Image Processing II*, 1987.
[126] S. Suzuki and K. Abe, "New fusion operations for digitized binary images and their applications," *IEEE Trans. Pattern Anal. Mach. Intell.*, PAMI-7, Nov. 1985, pp. 638–651.
[127] H. D. Tagare and R. J. P. de Figueiredo, "Order filters," *Proc. IEEE*, 73, pp. 163–165, Jan. 1985.
[128] S. L. Tanimoto, "A hierarchical cellular logic for pyramid computers," *J. Parallel Distrib. Comput.*, 1, 105–132, 1984.
[129] J. W. Tukey, *Exploratory Data Analysis*. Reading, MA: Addison-Wesley, 1977.
[130] S. G. Tyan, "Median filtering: Deterministic properties," in *Two-Dimensional Digital Signal Processing II: Transforms and Median Filters*, T. S. Huang, Ed. New York: Springer-Verlag, 1981.
[131] L. J. van Vliet, I. T. Young, and G. L. Beckers, "A nonlinear Laplace operator as edge operator in noisy images," *Comp. Vision Graph. Image Process.*, **45**, pp. 167–195, 1989.
[132] R. C. Vogt, "Morphological operator distributions based on monotonicity and the problem posed by digital disk-shaped structuring elements," in *Proc. SPIE 938*, 1988.
[133] S. H. Unger, "A computer oriented to spatial problems," *Proc. IRE*, vol. 46, pp. 1744–1750, 1958.
[134] P. D. Wendt, E. J. Coyle, and N. C. Gallagher, "Stack filters," *IEEE Trans. Acoust., Speech, Signal Process.*, ASSP-34, pp. 898–911, Aug. 1986.
[135] M. Werman and S. Peleg, "Min-max operators in texture analysis," *IEEE Trans. Pattern Anal. Mach. Intell.*, PAMI-7, Nov. 1985, pp. 730–733.
[136] A. S. Willsky, *Digital Signal Processing and Control and Estimation Theory: Points of Tangency, Areas of Intersection and Parallel Directions*. Cambridge, MA: MIT Press, 1979.
[137] A. Witkin, "Scale-space filtering," in *Proc. IJCAI*, Carlsrue, W. Germany, 1983.
[138] I. T. Young, "Modern digital image analysis," in *Proc. IEEE ICASSP-89*, Glasgow, Scotland, May 1989.
[139] A. Yuille, personal communication, 1989.
[140] A. Yuille and T. Poggio, "Scaling theorems for zero crossings," *IEEE Trans. Pattern. Anal. Mach. Intellig.*, PAMI-8, pp. 15–25, Jan. 1986.
[141] A. Yuille, D. Cohen, and P. Hallinan, "Face recognition by deformation templates," in *Proc. IEEE Conf. CVPR-89*, San Diego, CA, June 1989.
[142] L. A. Zadeh, "Fuzzy sets," *Inform. Control*, 8, 338–353, 1965.
[143] Z. Zhou and A. N. Venetsanopoulos, "Morphological skeleton representation and shape recognition," in *Proc. IEEE ICASSP-88*, New York, Apr. 1988.
[144] D. Casasent and E. Botha, "Optical symbolic substitution for morphological transformations," *Appl. Optics*, vol. 27, pp. 3806–3810, Sept. 1988.
[145] S. S. Wilson, "Morphological networks," in *Proc. SPIE*, vol. 1199: Visual Communications and Image Processing IV, Nov. 1989.

Petros Maragos (Member, IEEE) was born in Kalymnos, Greece, in 1957. He received the Diploma degree in electrical engineering from the National Technical University of Athens, Greece, in 1980, and the M.S.E.E. and Ph.D. degrees from the Georgia Institute of Technology, Atlanta, in 1982 and 1985, respectively.

From 1980 to 1985 he was a Research Assistant at the Digital Signal Processing Lab of the Electrical Engineering School at

Georgia Tech. In 1985 he joined the Faculty of the Division of Applied Sciences at Harvard University, Cambridge, where he is currently an Associate Professor of Electrical Engineering. He teaches and conducts research in the general areas of signal processing, image processing and computer vision, speech processing and recognition, and neural networks.

Dr. Maragos received a National Science Foundation Presidential Young Investigator Award in 1987. In 1989 he received the IEEE Acoustics, Speech, and Signal Processing Society's Paper Award for a publication in the Transactions of the Society. He is currently serving as an Associate Editor for the *IEEE Transactions on Acoustics, Speech, and Signal Processing*.

Ronald W. Schafer (Fellow, IEEE) received the B.S.E.E. and M.S.E.E. degrees from the University of Nebraska, Lincoln, in 1961 and 1962 respectively, and the Ph.D. degree from the Massachusetts Institute of Technology, Cambridge, in 1968.

From 1968 to 1974 he was a member of the Acoustics Research Department, Bell Laboratories, Murray Hill, New Jersey, where he was engaged in research on speech analysis and synthesis, digital signal processing techniques, and digital waveform coding. Since 1974 he has been on the faculty of the Georgia Institute of Technology as John O. McCarty Professor and Regents' Professor of Electrical Engineering. He is coauthor of the widely used textbooks, *Digital Signal Processing, Digital Processing of Speech Signals*, and the new text *Discrete-Time Signal Processing*. He has been active in the affairs of the IEEE Acoustics, Speech, and Signal Processing Society, having served as Associate Editor of the Transactions, member of several committees, Vice-President and President of the Society, and Chairman of the 1981 ICASSP.

Dr. Schafer is a Fellow of the IEEE and the Acoustical Society of America and he is a member of Sigma Xi, Eta Kappa Nu, and Phi Kappa Phi. He was awarded the Achievement Award and the Society Award of the IEEE ASSP Society in 1979 and 1983 respectively; the 1983 IEEE Region III Outstanding Engineer Award; and he shared the 1980 Emanuel R. Piore Award with L. R. Rabiner. In 1985 he received the Class of 1934 Distinguished Professor Award at Georgia Tech.